

A detailed exploration of the EDGES 21 cm absorption anomaly and axion-induced cooling

Chuang Li^{a,*}, Nick Houston^{b,†}, Tianjun Li^{c,d,‡}, Qiaoli Yang^{e,§} and Xin Zhang^{f,g,¶}

^a *College of Mechanical and Electrical Engineering, Wuyi University, Nanping 354300, China*

^b *Faculty of Science, Beijing University of Technology, Beijing 100124, China*

^c *CAS Key Laboratory of Theoretical Physics, Institute of Theoretical Physics, Chinese Academy of Sciences, Beijing 100190, China*

^d *School of Physical Sciences, University of Chinese Academy of Sciences, No. 19A Yuquan Road, Beijing 100049, China*

^e *Siyuan Laboratory and Physics Department, Jinan University, Guangzhou 510632, China*

^f *Key Laboratory of Computational Astrophysics, National Astronomical Observatories, Chinese Academy of Sciences, 20A Datun Road, Chaoyang District, Beijing 100012, China*

^g *School of Astronomy and Space Science, University of Chinese Academy of Sciences, No. 19A Yuquan Road, Beijing 100049, China*

The EDGES collaboration's observation of an anomalously strong 21 cm absorption feature around the cosmic dawn era has energised the cosmological community by suggesting a novel signature of dark matter in the cooling of cosmic hydrogen. In a recent letter we have argued that by virtue of the ability to mediate cooling processes whilst in the condensed phase, a small amount of axion dark matter can explain these observations within the context of standard models of axions and axion-like particles. These axions and axion-like particles (ALPs) can thermalize through gravitational self-interactions and so eventually form a Bose-Einstein condensate (BEC), whereupon large-scale long-range correlation can produce experimentally observable signals such as these. In this context the EDGES best-fit result favours an axion-like-particle mass in the (6, 400) meV range. Future experiments and galaxy surveys, particularly the International Axion Observatory (IAXO) and EUCLID, should have the capability to directly test this scenario. In this paper, we will explore this mechanism in detail and give more thorough computational details of certain key points.

* lichuang_physics@163.com

† nhouston@bjut.edu.cn, corresponding author

‡ tli@itp.ac.cn

§ qiaoli_yang@hotmail.com

¶ zhangxin@nao.cas.cn

Contents

I. Introduction	2
II. Astrophysics background	3
II.A. The 21 cm signal	3
II.B. Detection mechanism	4
II.C. Detection instruments and the EDGES observation	5
III. Axion physics	5
III.A. Basic properties	6
III.B. The axion as dark matter	8
III.B.1. The axion field in the early Universe	8
III.B.2. The condensation of axion dark matter	9
IV. Hydrogen cooling induced by axion condensation	14
V. Numerical computation and experimental constraints	17
V.A. The mass and relic density constraint	18
V.B. The mass and coupling constraint	19
VI. Summary	20
References	22

I. Introduction

In the standard cosmology, our present Universe arose from a hot soup of radiation and matter left over after the big bang. After the first 300,000 years elapsed, sufficient cooling allowed free electrons and protons to combine to form neutral hydrogen atoms and thus begin the cosmological dark ages, an epoch in which there were no luminous sources. Over time, local overdensities collapsed to form the first generations of stars and galaxies, resulting in the so-called cosmic dawn. As time went on this process continued, rendering the universe fully reionized, and ultimately resulting in today's almost transparent intergalactic medium dotted with galaxies, quasars and galaxy clusters.

Although our understanding of cosmology has advanced significantly over the last decades, many aspects of this cosmic dawn are still unexplored. Meanwhile, in the standard Λ CDM cosmology, this epoch is relatively predictable and easily understood. As such, it can serve as a ideal probe of physics beyond the Λ CDM paradigm.

One key observable is related to the absorption or emission spectrum of cosmic microwave background radiation at the cosmic dawn, arising from the neutral hydrogen present absorbing wavelengths close to atomic transitions, and thereby imprinting a characteristic spectral distortion in the vicinity of 21 cm, by virtue of the singlet/triplet spin flip transition. This feature redshifts to about 80 MHz today, and has been observed by the Experiment to Detect the Global Epoch of reionization Signature (EDGES) Collaboration [1], who claim that the effective 21 cm brightness temperature is:

$$T_{21} \simeq -0.52^{+0.18}_{-0.42} \text{ K}, \quad (1)$$

where the uncertainties quoted are at 99% confidence level.

The amplitude of this signal, fully described by subsequent Eq.(6), is given here in simple terms as

$$T_{21} \simeq 35\text{mK} \left(1 - \frac{T_\gamma}{T_s}\right) \sqrt{\frac{1+z}{18}}, \quad (2)$$

where T_s is the singlet/triplet spin temperature(see Eq.(4) for the exact definition) of the hydrogen gas present at that time, and T_γ is the CMB temperature. Once stellar emission of UV radiation begins, perhaps around $z \sim 20$, we expect that $T_\gamma \gg T_s \gtrsim T_{\text{gas}}$, due to the decoupling of hydrogen gas and the CMB at earlier times, and the

coupling of the spin temperature to the kinetic gas temperature around this period. In the standard Λ CDM scenario, $T_\gamma|_{z \sim 17} \simeq 49$ K and $T_{\text{gas}}|_{z \sim 17} \simeq 6.8$ K, so by Eq.(2), we have

$$T_{21} \gtrsim -0.21 K. \quad (3)$$

The significance of the EDGES deviation from the Λ CDM expectation is estimated to be 3.8σ , which represents an anomalously strong 21cm absorption feature from $z \in (20, 15)$, corresponding to the era of early star formation.

Explanations of the EDGES result proposed in the literature can be roughly classified into four types. Firstly, new mechanisms for cooling the gaseous medium, such as in Refs. [2–5, 7–10, 12, 13] by some kind of dark matter or [6, 11] by dark energy. Secondly, proposals adding an extra soft photon component to promote the CMB temperature, such as in Refs. [14–20]. Thirdly, modifications of cosmological evolution process, such as in Refs. [21, 22]. Lastly, improvements to the measurement and treatment of the foregrounds to relax the anomaly, such as in Refs. [23, 24].

We are interested in the first of these approaches, but the interaction cross section required to achieve this is prohibitive for most models of dark matter [2]. To be consistent with other experimental and observational constraints, models capable of explaining the EDGES observation require millicharged dark matter comprising just 0.3 – 2% of the total dark matter abundance, with masses and millicharges in the (10, 80) MeV and (10^{-4} , 10^{-6}) ranges, respectively [3–5].

As such, in the following we will propose a more natural dark-matter theoretic approach, which is based on the speculated ability of axion dark matter to form a Bose-Einstein Condensate [25, 26]. In many respects, this condensed state behaves as ordinary CDM (Cold Dark matter), but it has a particularly interesting ability to induce transitions between momentum states of coupled particle species, and hence is naturally equipped with a cooling effect. This mechanism was originally invoked in Ref. [27] to lower the photon temperature in the era of Big Bang Nucleosynthesis (BBN), albeit with a different motivation to our own ¹.

By consistently adjusting the parameter range, we can analogously lower the hydrogen temperature prior to the cosmic dawn to explain the EDGES observations in the context of axion and axion-like-particle (ALP) models. We fortunately find that, to be close to the existing experimental limits, the implied parameter range could be tested at the next generation of axion experiments and large scale surveys, particularly IAXO[28] and EUCLID[29].

This paper is intended to serve as an extended edition of a previous letter “Natural explanation for 21 cm absorption signals via axion-induced cooling” [9]. As such the content will be similar, but we will provide more background and detailed computational steps.

We emphasize for clarity that, although several other axion-related explanations [8, 18, 19] have been proposed, our approach differs in many essential respects from them. We also note Ref. [10], which appeared shortly after Ref. [9] deals with the same scenario of axion BEC-induced cooling and 21 cm cosmology, but with different emphasis.

The outline of this paper is as follows. In Section II, we give a concise introduction of the astrophysics background, including 21 cm cosmology and the EDGES experiment. In Section III, we give an overview of the relevant aspects of axion physics, covering the basic motivation of the axion proposal, the axion dark matter scenario, and the Bose-Einstein condensation of axion dark matter. In Section IV, the hydrogen cooling mechanism is explored in detail, based on the axion BEC, including concrete cooling rate formulae. In Section V, we demonstrate the resulting parameter space constraints, and discuss the possible experiments and observations with the potential to confirm this model. Section VI provides a summary.

II. Astrophysics background

II.A. The 21 cm signal

The so-called 21 cm signal/line is associated to the hyperfine splitting between the spin singlet and triplet states of the electron and proton in a hydrogen atom. Hydrogen is ubiquitous in the Universe, amounting to $\sim 75\%$ of the gas mass present in the intergalactic medium (IGM). As such, this observable provides a convenient tracer of the properties of the first billion years of our Universe. The 21 cm line from gas during this time redshifts to 30-200 MHz today, making it a prime target for the new generation of radio interferometers currently being built. The related research is an active area of astrophysics and cosmology, often referred to simply as ‘21 cm cosmology’ [30, 31].

¹ Concretely, the authors of [27] wanted to ease the discrepancy between the observed and predicted primordial ^7Li abundance by adjusting the baryon-to-photon ratio.

There are two kinds of 21 cm signal, full 3D and global (sky-averaged), respectively. For the full 3D signal, observations of the 21 cm line constrain the properties of the intergalactic medium and the cumulative impact of light from all galaxies. In combination with other direct observations of the sources, they provide a powerful tool for learning about the first stars and galaxies. By observing the surrounding ionization bubbles, they can also provide useful information about active galactic nuclei (AGN), such as quasars. Because part of the signal couples with the density field, which can give some information about the initial conditions of cosmic inflation and neutrino masses in the form of the power spectrum, it could also allow precise measurements of cosmological parameters, thereby illuminating fundamental physics.

Besides the above physical significance of the full 3D 21 cm signal, Ref. [34–36] has also shown that the global (sky-averaged) 21 cm observations can be used to constrain for example the Lyman- α background intensity and heat deposition, the growth rate of dark matter halos, and to provide unique signatures of Population III stars.

II.B. Detection mechanism

The detectability of the 21 cm signal relies on the spin temperature, an effective temperature that describes the relative abundances of the ground and excited states of the hyperfine splitting of the hydrogen atom, defined by

$$n_1/n_0 = (g_1/g_0) \exp(-T_\star/T_s), \quad (4)$$

where n_i are the number densities of hydrogen atoms in the two hyperfine levels, subscript 0 and 1 for the $1S$ singlet and $1S$ triplet levels, respectively, g_i is the statistical degeneracy factors of the two levels, with $(g_1/g_0) = 3$, and $T_\star \equiv hc/k\lambda_{21\text{cm}} = 0.068\text{ K}$. This signal can only be observed when the spin temperature deviates from a given background.

In the early Universe when the gas density is high, collisions between different particles may induce spin-flips in a hydrogen atom and dominate the spin temperature coupling². Then the spin temperature can be identified with the background gas temperature, which is the same as the CMB temperature.

For most of the redshifts $z \leq 200$, gas collisional coupling of the 21 cm line is inefficient, and absorption/emission of 21 cm photons to and from the radio background, primarily the CMB, becomes the most important element affecting the spin temperature, so the spin temperature is close to the CMB temperature.

However, when the first generations of stars begin to form (around $z \sim 20$), Ly α photons offer another coupling channel via the so-called Wouthuysen-Field effect [32, 33]. The main idea is as follows: suppose that hydrogen is initially in the hyperfine singlet state, so that absorption of a Ly α photon will excite the atom into higher energy level, such as either of the central 2P hyperfine states. From here, the transition to a lower energy level can place the atom in either of the two ground state hyperfine levels (i.e., the spin singlet and triplet states). If the final state is triplet then a spin-flip has occurred. Hence, Ly α photons can induce spin-flips via an intermediate excited state.

As a whole, the spin temperature is determined by three processes: (i) collisions with other hydrogen atoms, electrons and protons; (ii) absorption/emission of 21 cm photons to and from the CMB; (iii) scattering of Ly α photons. The resulting spin temperature is then set by the equilibrium balance of these effects³, formulated as

$$T_s^{-1} = \frac{T_\gamma^{-1} + x_\alpha T_\alpha^{-1} + x_c T_K^{-1}}{1 + x_\alpha + x_c}, \quad (5)$$

where T_γ is the temperature of CMB, T_α is the color temperature of the Ly α radiation, T_K is the gas kinetic temperature, T_α is closely coupled to T_K from the repeated recoil and scattering, and x_α, x_c are the coupling coefficients due to scattering of Ly α photons and atomic collisions, respectively [33]. Obviously, the spin temperature will be very close to T_γ when $x_\alpha + x_c \ll 1$ and approaches the gas temperature when $x_\alpha + x_c \gg 1$.

Roughly speaking, shortly after the decoupling of the CMB and hydrogen gas at $z \sim 200$, T_s is between T_γ and T_H ; as the Universe expands, diluting the gas, T_s moves towards T_γ . Around $z \sim 20$, stars begin the emission of Ly α and X-ray photons, and T_s couples to the hydrogen gas temperature due to the Wouthuysen-Field effect. So we expect that $T_\gamma \gg T_s \gtrsim T_{\text{gas}}$ at $z \sim 20$.

To be used conventionally with observations, Ref. [30] also defines an effective 21 cm brightness temperature

$$T_{21} = 26.8 x_{\text{HI}} \frac{\rho_g}{\bar{\rho}_g} \left(\frac{\Omega_b h}{0.0327} \right) \left(\frac{\Omega_m}{0.307} \right)^{-1/2} \left(\frac{1+z}{10} \right)^{1/2} \left(\frac{T_s - T_\gamma}{T_s} \right) \text{ mK} \quad (6)$$

² There exist three main channels: collisions between two hydrogen atoms, collisions between a hydrogen atom and an electron, and similarly, collisions between a hydrogen atom and a proton.

³ The equilibrium condition is an excellent approximation since the rate of these processes is much faster than the de-excitation time of the 21 cm line.

where x_{HI} is the mean mass fraction of hydrogen that is neutral (i.e. not ionized), ρ_g is the gas density and $\bar{\rho}_g$ its cosmic mean value, Ω_m and Ω_b are the cosmic mean densities of matter and of baryons, respectively, in units of the critical density, h is the Hubble parameter in units of $100 \text{ km s}^{-1} \text{ Mpc}^{-1}$, z is the redshift (corresponding to an observed wavelength of $21 \times (1+z) \text{ cm}$ and an observed frequency of $1420/(1+z) \text{ MHz}$), $T_\gamma = 2.725 \times (1+z)$ is the CMB temperature at z , and T_s is the spin temperature of hydrogen at z as shown in Eq.(5).

II.C. Detection instruments and the EDGES observation

As we have shown in the previous section, detecting the 21 cm signal from the cosmic dawn should enable key insights into the nature of the first stellar objects and their substantial influence on galaxy formation, and the later processes which lead to the complex structures we see in the Universe today. The instruments to do so are roughly classified in two ways: full 3D signal detection instruments, and global signal detection instruments. The global signal can be viewed as a zeroth order approximation to the full 3D signal, as it is averaged over large angular scales.

Because of the spatial variation in the different radiation fields and properties of the IGM, the full 3D signal will be highly inhomogeneous. There are many full 3D signal detection instruments, such as the Giant Meterwave Radio Telescope (GMRT)[37, 38], Primeval Structure Telescope (PAST or 21CMA)[39], Murchison Widefield Array (MWA)[40, 41], the LOw Frequency ARray (LOFAR)[42], and the Precision Array to Probe the Epoch of Reionization (PAPER)[43], which aim to detect the fluctuations of the redshifted 21 cm radio background induced by variations in the neutral hydrogen density. Next generation instruments, such as SKA [44–49], will be able to make more detailed observation of the ionized regions during reionization, and probe more of the properties of cosmic hydrogen.

The global 21 cm signal is averaged over the sky without high angular resolution, so it can be detected as an absolute frequency-dependent temperature via a single dipole antenna. The pioneering experiments aiming to do so are the Sonda Cosmológica de las Islas para la Detección de Hidrógeno Neutro (SCI-HI)[50], the Large-Aperture Experiment to Detect the Dark Ages (LEDA)[51], the Shaped Antenna measurement of the background Radio Spectrum 2 (SARAS 2)[52], the COsmological Reionization Experiment (CORE)[53], the Probing Radio Intensity at high z from Marion (PRIZM)[54], and the Experiment to Detect the Global EoR Signature (EDGES)[1, 2].

EDGES is a collaboration between Arizona State University and the MIT Haystack Observatory, funded by the National Science Foundation (NSF). The project's goal is to detect the radio signatures of hydrogen from the cosmic period known as the Epoch of Reionization (EoR), soon after the formation of the first stars and galaxies. Concretely, EDGES aims to probe the radiative properties of the first stars and compact objects via the profile of the observed 21 cm absorption or emission spectrum features in the radio background.

Although the detection principle is simple, a practical measurement is complicated by the need for nontrivial subtraction of galactic foregrounds, which are orders of magnitude larger than the expected signal. On the assumption of spectral smoothness of the foreground signals, in contrast to the specific spectral structure of the 21 cm absorption profile, foregrounds can be predicted by, for example, fitting a low order polynomial, which once subtracted leaves the desired 21 cm signal in the residuals [55]. In foreground estimation an additional complication is the Earth's ionosphere, which affects the propagation of radio waves via absorption of incoming radiation, and direct thermal emission from electrons in the ionosphere. This contribution can however also be modeled with a good fit to the data [56]. To account for possible mixing with the foregrounds, precise calibration of the instrumental frequency response is also required, which is a significant milestone completed by the EDGES collaboration [57]. Note: While the present paper was being completed, a new controversy about foreground model consistency appeared[58], however the response of EDGES collaboration is substantive[59]. With global 21 cm signal model[31], EDGES can then perform least-squares and/or Markov Chain Monte Carlo (MCMC) analyses to get best-fits and reasonable confidence intervals, and consequently derive astrophysical information from observations through parameter estimation in these calibrated and integrated model fits [60, 61].

III. Axion physics

In this section we will give a brief overview of the relevant aspects of axion physics and cosmology, further details are available in Ref. [62–64].

III.A. Basic properties

The axion is a hypothetical elementary particle originally postulated in 1977 [65–67] to resolve the strong CP problem in quantum chromodynamics (QCD). The existence of axion like particles (ALPs) are more generally predictions of many high energy physics models, including string theory in particular. In the following, the QCD axion is contrasted with ALPs, while we use the term ‘axion’ flexibly to include both the QCD axion and ALPs.

The QCD axion

The QCD axion primarily provides a excellent solution to the strong CP problem, and thus an attractive target for particle physics searches beyond the Standard Model[65–71]. The basic idea is concisely described as follows. The QCD vacuum is non-trivially dependent on a parameter $\theta \in [0, 2\pi]$, which results an effective CP odd term to the QCD Lagrangian,

$$\mathcal{L}_\theta = \frac{\theta}{32\pi^2} G_{\mu\nu}^a \tilde{G}^{\mu\nu a}, \quad (7)$$

where $G_{\mu\nu}^a$ is the gluon field strength tensor, and $\tilde{G}^{\mu\nu a} = \epsilon^{\mu\nu\alpha\beta} G_{\alpha\beta}^a / 2$ is its dual. This θ term can be changed by adding additional phases to the quark mass matrix via $q_i \rightarrow e^{i\alpha_i \gamma_5/2} q_i$, and so the physical parameter that determines the CP violation in QCD is $\tilde{\theta}$,

$$\tilde{\theta} = \theta - \sum \alpha_i, \quad (8)$$

or

$$\tilde{\theta} = \theta + \arg \det M_u M_d, \quad (9)$$

where M_u, M_d are the quark mass matrices.

The term $\mathcal{L}_{\tilde{\theta}}$ allows P and T or CP violation, but since CP is conserved well in QCD processes, we infer that $|\tilde{\theta}| \lesssim 10^{-10}$ [72, 73]. This fine tuning constitutes the strong CP problem.

The first solution is proposed by Peccei & Quinn [65], which introduced an $U(1)$ symmetry (PQ symmetry), and a scalar (the PQ scalar) which dynamically leads to $\tilde{\theta} \simeq 0$ due to the effects of a potential for $\tilde{\theta}$ arising from QCD instanton effects. Later this model was complemented by Wilczek & Weinberg by implementing the same mechanism (the PQ mechanism) in the realistic Weinberg-Salam model [66, 67], where they realized that the spontaneous breaking of PQ symmetry results in a pseudo-Goldstone boson, coined the axion by Wilczek. The above Peccei-Quinn-Wilczek-Weinberg (PQWW) model was excluded by experiment quickly, but the PQ mechanism was subsequently implemented by other models, the most important of which are the following two.

- The Kim-Shifman-Vainshtein-Zakharov (KSVZ) [68, 69] axion model, which adds the PQ scalar and a heavy quark to the Weinberg-Salam model.
- The Dine-Fischler-Srednicki-Zhitnitsky (DFSZ) [70, 71] axion model, which adds the PQ scalar and an additional Higgs field to the Weinberg-Salam model.

The PQ mechanism is also endorsed by a theorem of Vafa and Witten [74] which claims that the vacuum energy of the QCD instanton potential is minimized at the CP conserving value.

To be more specific, here we will follow the literature [131–133], to present the PQ mechanism briefly. The complex PQ scalar field is expressed as:

$$S = \rho \exp \left(i \frac{\phi}{f_a} \right), \quad (10)$$

where ρ is the radial field, ϕ is the angular field, and $f_a = \langle S \rangle$ is the energy scale of PQ symmetry breaking. After PQ symmetry breaking, ϕ is the massless Goldstone boson of this broken symmetry, axion. ρ is generally massive and decouples, so the Lagrangian changes to:

$$L_{\text{total}} = L_{\text{SM}} - \frac{1}{2} \partial_\mu \phi \partial^\mu \phi + L_{\text{int}}[\partial^\mu \phi / f_a; \Psi] + \left(\bar{\theta} + \mathcal{C} \frac{\phi}{f_a} \right) \frac{g^2}{32\pi^2} F_a^{\mu\nu} \tilde{F}_{a\mu\nu}. \quad (11)$$

where \mathcal{C} is known as the colour anomaly of the PQ symmetry, and is given by

$$\mathcal{C} \delta_{ab} = 2 \text{Tr } Q_{\text{PQ}} T_a T_b. \quad (12)$$

Here the trace is over all the fermions in the theory, and T_a are the generators of the corresponding fermion representations. The colour anomaly also represents the number of potential vacua in the range $[0, 2\pi f_a]$, is thus also known as the domain wall number, which must be integer [102].

The last term is from the PQ symmetry chiral anomaly, which also leads to an induced axion potential, $V_{\text{eff}}(\phi)$. The dynamics of ϕ send it to one of these vacua, which is the essence of the PQ mechanism,

$$\left\langle \frac{\partial V_{\text{eff}}}{\partial \phi} \right\rangle = -\frac{\xi}{f_a} \frac{g^2}{32\pi^2} \left\langle F_a^{\mu\nu} \tilde{F}_{a\mu\nu} \right\rangle \Big|_{\langle \phi \rangle = -\frac{f_a}{C} \bar{\theta}} = 0. \quad (13)$$

More concretely,

$$V_{\text{eff}} \sim 1 - \cos\left[\bar{\theta} + C \frac{\langle \phi \rangle}{f_a}\right]. \quad (14)$$

So, $\langle \phi \rangle = -\frac{f_a}{C} \bar{\theta}$ will minimize $V_{\text{eff}}(\phi)$.

In the following paper, unless otherwise stated the colour anomaly will be absorbed into f_a .

For the small ϕ displacements from the potential minimum, the potential can be expanded as a Taylor series. The dominant piece is the mass term:

$$V_{\text{eff}}(\phi) \approx \frac{1}{2} m_a^2 \phi^2 \quad \text{or} \quad m_a^2 = \left\langle \frac{\partial^2 V_{\text{eff}}}{\partial \phi^2} \right\rangle. \quad (15)$$

Furthermore, the mass is given by:

$$m_a = \Lambda_a^2 / f_a \approx 6 \times 10^{-6} \text{eV} \left(\frac{10^{12} \text{GeV}}{f_a} \right), \quad (16)$$

where Λ_a is a non-perturbative scale induced by QCD instantons. Typically the PQ symmetry breaking scale f_a is much higher than Λ_a , so axion gets a small mass. In addition, axion self-interactions and interactions with Standard Model fields are also suppressed by powers of f_a . By virtue of the underlying shift symmetry $\phi \rightarrow \phi + \text{const}$, the axion mass is protected from perturbative quantum corrections. In general, the axion mass will also be temperature dependent, because of the temperature dependence of the non-perturbative effects. All of these elements conspire to make the axion a light, weakly interacting, long-lived particle, and hence a natural dark matter candidate ⁴.

There are of course newer variant models with some enhancements, designed to avoid issues such as Landau poles, or astrophysical limits, etc. [75–77], or to incorporate PQ symmetry with some kinds of supersymmetric standard model or grand unified theory [78–81], or to get Peccei-Quinn symmetries from exact discrete symmetries [82], or to unify PQ symmetry and neutrino seesaw mechanism [83, 84], which overall give more flexible theoretical configurations.

Axion-like particles

Any breaking of anomalous global symmetries will result in some pseudo Nambu-Goldstone (pNG) bosons, if these bosons have similar properties to the QCD axion we will refer them as axion-like particles (ALPs). There are some notable examples, such as lepton number symmetry breaking [85, 86] or family/flavor symmetry breaking [87–90], but the most interesting situation we should mention is that ALPs commonly exist in the string theory framework [91–93].

As is well known, extra spacetime dimensions are introduced in string theory for self-consistency. These additional dimensions are typically compactified to very small size manifolds (usually of “Calabi-Yau” type) to be compatible with our 4D world.

In the low energy effective description of string theory, the zero modes of the antisymmetric tensors on the compactified manifolds have similar properties to QCD axions [91, 95]. For example, they are pseudoscalar, they have axion-like couplings (to $G_{\mu\nu}^a \tilde{G}^{\mu\nu a}$), they are massless to all orders in perturbation theory, and they can obtain a small mass via a non-perturbative instanton potential. So, they are called axion-like particles. From the point of view of phenomenology, the key differences between the QCD axion and axion-like particles are the coupling strengths to the standard model particles.

⁴ These properties also permit axions to address problems of inflation or dark energy, which are out of our present scope.

III.B. The axion as dark matter

Dark matter (DM) is a critical element of the modern standard model of cosmology. If the QCD axion exists and the decay constant f_a in Eq.(16) is large, it should be extremely weakly interacting and stable, and thus an excellent DM candidate [97–101]. Whilst the literature on this topic is abundant, we will in the following focus purely on the elements which are of relevance to our later discussion.

III.B.1. The axion field in the early Universe

For the axion field in the early Universe, there are several entangled factors of relevance. For a clear description, we briefly delineate these into three parts as follows.

Productions of axions

As mentioned in the previous section, the evolution of axions in the early Universe is determined by the PQ mechanism: PQ symmetry breaking to make the axion possible and QCD instanton effects to give the axion mass. Here we will concentrate on the production of a cosmic axion population, which primarily is expected to occur in the following ways.

- Thermal axion production

Just as for other massive standard model particles, the mutual production and annihilation during reheating can result in a thermal relic population of QCD axions. Concretely, QCD axions are produced from the standard model plasma typically by pion scattering, and decouple or freeze-out when the rate of the process $\pi + \pi \rightarrow \pi + a$ becomes lower than the Hubble rate. The thermal axion abundance is determined by the decoupling temperature, with a roughly inverse relation, see e.g. Ref. [113].

ALPs are generically more weakly coupled to the standard model than the QCD axion, and their abundance is model dependent, with enough freedom to adjust. If ALPs arise in models with SUSY and extra dimensional compactifications (mainly string theory), a generic prediction states that the axion field can be coupled to a massive particle, U , with $m_U > m_a$. As U decays, a population of relativistic ALPs is created [105–109]. This scenario is a kind of dark radiation with a rich phenomenology, but it is not the emphasis of our paper.

- Cold axion production

Various kinds of topological defects can be formed during the breaking of global symmetries [110]. In our case of a global $U(1)$ PQ symmetry, this gives rise to global axionic strings and domain walls (if [NH: the] colour anomaly $\mathcal{C} > 1$, the domain walls are stable, otherwise unstable). If PQ symmetry is broken after inflation, these topological defects can decay to produce a population of cold axions. But some other mechanism are typically needed to eliminate the domain wall problem [111, 112].

In the scenario where PQ symmetry is broken before inflation, topological defects and their decay products are inflated away, and thus can be neglected.

Another method of cold axion production is vacuum realignment or misalignment⁵, which relies only on the basic properties of the axion.

In an FLRW universe the equation of motion of the axion field is given by

$$\ddot{\phi} + 3H\dot{\phi} - \frac{1}{a^2} \nabla^2 \phi + V'_{eff}(\phi) = 0. \quad (17)$$

In the early Universe, we can reasonably assume the axion scalar field is uniformly distributed in space (i.e., homogeneous), then the spatial derivatives disappear, if we further take only the mass term in the effective potential for simplicity, we can get

$$\ddot{\phi} + 3H\dot{\phi} + m_a^2 \phi = 0. \quad (18)$$

⁵ Here, “vacuum realignment” means the process that axion field relaxes to the potential minimum, and “misalignment” means the coherent initial displacement of the axion field

which is similar to the equation of a simple harmonic oscillator with time-dependent friction. Furthermore, with $H(t_i) \gg m_a$, the initial conditions are well defined⁶:

$$\phi(t_i) = f_a \theta_{a,i}, \quad \dot{\phi}(t_i) = 0. \quad (19)$$

Hence, the misalignment production of axions is determined by Eqs. (18), (19), while the coherent initial displacements of the axion field depends specifically on if PQ symmetry breaking occurs before or after inflation [62].

III.B.2. The condensation of axion dark matter

After becoming massive, axions may intuitively evolve like ordinary dark matter, without special phenomena. But thanks to the bosonic nature of axions and their very high phase space density, a number of novel condensation-derived effects have been suggested to occur [25–27, 114–116], as we will explore in this section.

We note firstly that the underlying conditions for BEC formation are that: (i) the system comprise a large number of identical bosons, (ii) the bosons are conserved in number, (iii) the system are sufficiently degenerate and (iv) the system are in sufficient thermal equilibrium [116]. CDM axions satisfy all the conditions (from the following derivation), making the formation of a BEC a reasonable possibility. Dark matter axions may thermalize in the early universe by two kinds of processes[26]: intrinsic self-interactions of the $\lambda\phi^4$ type and gravitational self-interactions. Once thermalized, they can form a Bose-Einstein condensate.

Axion interactions

Inside a cubic box of volume $V = L^3$ with periodic boundary conditions, we expand the axion field $\phi(\vec{x}, t)$ and its canonical conjugate field $\pi(\vec{x}, t)$ into Fourier components in the Heisenberg picture as

$$\begin{aligned} \phi(\vec{x}, t) &= \sum_{\vec{n}} \left(a_{\vec{n}}(t) \Phi_{\vec{n}}(\vec{x}) + a_{\vec{n}}^\dagger(t) \Phi_{\vec{n}}^*(\vec{x}) \right), \\ \pi(\vec{x}, t) &= \sum_{\vec{n}} (-i\omega_{\vec{n}}) \left(a_{\vec{n}}(t) \Phi_{\vec{n}}(\vec{x}) - a_{\vec{n}}^\dagger(t) \Phi_{\vec{n}}^*(\vec{x}) \right). \end{aligned} \quad (20)$$

where

$$\Phi_{\vec{n}}(\vec{x}) = \frac{1}{\sqrt{2\omega_{\vec{n}}V}} e^{i\vec{p}_{\vec{n}} \cdot \vec{x}} \quad (21)$$

and $\vec{n} = (n_1, n_2, n_3)$ with n_k ($k = 1, 2, 3$) integers, $\vec{p}_{\vec{n}} = \frac{2\pi}{L}\vec{n}$, and $\omega_{\vec{n}} = \sqrt{\vec{p}_{\vec{n}} \cdot \vec{p}_{\vec{n}} + m_a^2}$. The $a_{\vec{n}}$ and $a_{\vec{n}}^\dagger$ satisfy canonical equal-time commutation relations:

$$[a_{\vec{n}}(t), a_{\vec{n}'}^\dagger(t)] = \delta_{\vec{n}, \vec{n}'}, \quad [a_{\vec{n}}(t), a_{\vec{n}'}(t)] = 0. \quad (22)$$

In the Newtonian limit, neglecting high order self-interactions, the generic action density of axions is

$$\mathcal{L}_a = \frac{1}{2} \partial_\mu \phi \partial^\mu \phi - \frac{1}{2} m_a^2 \phi^2 + \frac{\lambda}{4!} \phi^4 + \frac{G}{2} \int d^3x d^3x' \frac{\rho(\vec{x}, t) \rho(\vec{x}', t)}{|\vec{x} - \vec{x}'|}, \quad (23)$$

where G is the Newtonian constant, $\rho = \frac{1}{2}(\pi^2 + m_a^2 \phi^2)$ is the axion energy density.

Provided the axions are non-relativistic (e.g. cold axions produced via the misalignment mechanism), energy conservation allows only axion number conserving processes at tree level, and so the intrinsic interactions of the axion field are

$$H_\lambda = \sum_{\vec{n}_1, \vec{n}_2, \vec{n}_3, \vec{n}_4} \frac{1}{4} \Lambda_{\lambda}^{\vec{n}_3, \vec{n}_4}_{\vec{n}_1, \vec{n}_2} a_{\vec{n}_1}^\dagger a_{\vec{n}_2}^\dagger a_{\vec{n}_3} a_{\vec{n}_4}, \quad (24)$$

where

$$\Lambda_{\lambda}^{\vec{n}_3, \vec{n}_4}_{\vec{n}_1, \vec{n}_2} = -\frac{\lambda}{4m_a^2 V} \delta_{\vec{n}_1 + \vec{n}_2, \vec{n}_3 + \vec{n}_4}. \quad (25)$$

⁶ At the time of PQ symmetry breaking the Hubble rate is much larger than the axion mass, so the field is overdamped and $\dot{\phi} = 0$ initially.

Neglecting general relativistic corrections and dropping again all axion number violating terms, for processes well within the horizon, the gravitational interactions of the axion fluid are described by

$$H_g = \sum_{\vec{n}_1, \vec{n}_2, \vec{n}_3, \vec{n}_4} \frac{1}{4} \Lambda_g^{\vec{n}_3, \vec{n}_4}_{\vec{n}_1, \vec{n}_2} a_{\vec{n}_1}^\dagger a_{\vec{n}_2}^\dagger a_{\vec{n}_3} a_{\vec{n}_4}, \quad (26)$$

where

$$\Lambda_g^{\vec{n}_3, \vec{n}_4}_{\vec{n}_1, \vec{n}_2} = -\frac{4\pi G m_a^2}{V} \delta_{\vec{n}_1 + \vec{n}_2, \vec{n}_3 + \vec{n}_4} \left(\frac{1}{|\vec{p}_{\vec{n}_1} - \vec{p}_{\vec{n}_3}|^2} + \frac{1}{|\vec{p}_{\vec{n}_1} - \vec{p}_{\vec{n}_4}|^2} \right). \quad (27)$$

To guarantee momentum conservation for each individual interaction, the Kronecker symbol $\delta_{\vec{n}_1 + \vec{n}_2, \vec{n}_3 + \vec{n}_4}$ is inserted in Eq. (25, 27).

Any axion number violating processes can be safely ignored because they occur only in loop diagrams at higher orders in an expansion in powers of $1/f_a$.⁷ Hence dropping all terms of the form $a^\dagger a^\dagger a^\dagger a^\dagger$, $a a^\dagger a^\dagger a^\dagger$, $a a a a$, and $a a a a^\dagger$ is quite reasonable.

Equivalent to a large number M of coupled oscillators, the Hamiltonian can be generically expressed as

$$H = \sum_{j=1}^M \omega_j a_j^\dagger a_j + \sum_{i,j,k,l} \frac{1}{4} \Lambda_{kl}^{ij} a_k^\dagger a_l^\dagger a_i a_j, \quad (28)$$

where $\Lambda = \Lambda_\lambda + \Lambda_g$, k, l, i, j represent $\vec{n}_k, \vec{n}_l, \vec{n}_i, \vec{n}_j$, and $\Lambda_{kl}^{ij} = \Lambda_{lk}^{ij} = \Lambda_{kl}^{ji} = \Lambda_{ij}^{kl}$.^{*} The total number of particles is

$$N = \sum_{l=1}^M \mathcal{N}_l = \sum_{l=1}^M a_l^\dagger a_l, \quad (29)$$

which is conserved, where $\mathcal{N}_l = a_l^\dagger a_l$.

After knowing the underlying dynamics of the axion field, the question of interest now is: starting with an arbitrary initial state, how quickly will the average occupation numbers $\langle \mathcal{N}_l \rangle = \langle a_l^\dagger a_l \rangle$ approach a thermally equilibrated distribution? The usual approach to answering this question relies upon a Boltzmann equation approach, which is however not valid for the cold axion fluid because of the different underlying assumptions. As such, a more general approach is required.

Supposing $l = 1 \dots M$, and we define

$$a_j(t) = (A_j + B_j(t)) e^{-i\omega_j t} + \mathcal{O}(\Lambda^2), \quad (30)$$

⁷ In fact, around the axion mass range of interest, all axion number violating processes will occur on time scales much longer than the age of the universe [26].

where $A_j \equiv a_j(0)$ and $B_j(t)$ are respectively zeroth and first order, and $B_j(0) = 0$, one finds that [26]

$$\begin{aligned}
\dot{\mathcal{N}}_l = & i \sum_{i,j,k=1}^M \frac{1}{2} (\Lambda_{ij}^{kl} A_i^\dagger A_j^\dagger A_k A_l e^{-i\Omega_{ij}^{kl}t} - h.c.) \\
& + \sum_{k,i,j=1}^M \frac{1}{2} |\Lambda_{ij}^{kl}|^2 [\mathcal{N}_i \mathcal{N}_j (\mathcal{N}_l + 1) (\mathcal{N}_k + 1) - \mathcal{N}_l \mathcal{N}_k (\mathcal{N}_i + 1) (\mathcal{N}_j + 1)] \frac{2}{\Omega_{ij}^{kl}} \sin(\Omega_{ij}^{kl}t) \\
& + \sum_{k,i,j=1}^M \sum_{\substack{p,m,n=1 \\ (p;m,n) \neq (k;i,j)}}^M \left[\frac{1}{2} \Lambda_{kl}^{ij} \Lambda_{mn}^{lp} A_m^\dagger A_n^\dagger A_k^\dagger A_p A_i A_j e^{i(\Omega_{ij}^{kl} + \Omega_{lp}^{mn}/2)t} \frac{1}{\Omega_{lp}^{mn}} \sin\left(\frac{\Omega_{lp}^{mn}}{2}t\right) + h.c. \right] \\
& + \sum_{k,i,j=1}^M \sum_{\substack{p,m,n=1 \\ (p;m,n) \neq (l;i,j)}}^M \left[\frac{1}{2} \Lambda_{kl}^{ij} \Lambda_{mn}^{kp} A_l^\dagger A_m^\dagger A_n^\dagger A_p A_i A_j e^{i(\Omega_{ij}^{kl} + \Omega_{kp}^{mn}/2)t} \frac{1}{\Omega_{kp}^{mn}} \sin\left(\frac{\Omega_{kp}^{mn}}{2}t\right) + h.c. \right] \\
& - \sum_{k,i,j=1}^M \sum_{\substack{p,m,n=1 \\ (p;m,n) \neq (j;l,k)}}^M \left[\frac{1}{2} \Lambda_{lk}^{ij} \Lambda_{ip}^{mn} A_l^\dagger A_k^\dagger A_p^\dagger A_m A_n A_j e^{i(\Omega_{ij}^{kl} + \Omega_{ip}^{mn}/2)t} \frac{1}{\Omega_{ip}^{mn}} \sin\left(\frac{\Omega_{ip}^{mn}}{2}t\right) + h.c. \right] \\
& - \sum_{k,i,j=1}^M \sum_{\substack{p,m,n=1 \\ (p;m,n) \neq (i;l,k)}}^M \left[\frac{1}{2} \Lambda_{lk}^{ij} \Lambda_{jp}^{mn} A_l^\dagger A_k^\dagger A_p^\dagger A_i A_m A_n e^{i(\Omega_{ij}^{kl} + \Omega_{jp}^{mn}/2)t} \frac{1}{\Omega_{jp}^{mn}} \sin\left(\frac{\Omega_{jp}^{mn}}{2}t\right) + h.c. \right], \\
& + \mathcal{O}(\Lambda^3)
\end{aligned} \tag{31}$$

where $\Omega_{ij}^{kl} \equiv \omega_k + \omega_l - \omega_i - \omega_j$, and \mathcal{N}_l is short for $\mathcal{N}_{\vec{p}_l}$. The double sums will be ignored in the following discussion.

The key quantity for discussions of axion condensation is the relaxation rate, defined as

$$\Gamma \sim \frac{\dot{\mathcal{N}}}{\mathcal{N}}, \tag{32}$$

which is time-dependent. As the relaxation rate reaches a value equal to or bigger than the Hubble rate, the system will approach thermal equilibrium.

Self-relaxation rate

Based on the relation between the relaxation rate and the energy associated to the corresponding transition, there are two possible regimes. This first condition: $\Gamma \ll \delta\omega$, defines the “particle kinetic regime”. In the particle kinetic regime, the first order terms in the evolution equations are irrelevant because they average out in time, and the second order terms dominate. The second condition: $\Gamma \gg \delta\omega$, defines the “condensed regime”. In the condensed regime, contrastingly, the first order terms not only exist but also dominate over the second order terms. As such we can use the first order equations to estimate the relaxation rate of the axion dark matter due to $\lambda\phi^4$ and gravitational self-interactions.

It will be useful to expand on these points in more detail.

• The particle kinetic regime

In this case the rate at which the occupation number of a typical oscillator changes is small compared to the energy exchanged in the corresponding transitions, and hence also $\Omega_{ij}^{kl}t \gg 1$. For the oscillator couplings of the axion field, Eqs. (25) and (27), as a general rule, whilst the global energy of the fluid is always conserved, local energy is not necessarily conserved in any one transition. Three-momentum is however conserved in each transition.

Not only the first order terms in Eq. (31), but also the second order terms in the double sums, average to zero in time.

The particle density in physical space is

$$n = \int \frac{d^3p}{(2\pi)^3} \mathcal{N}_{\vec{p}}, \tag{33}$$

and, if most states are unoccupied, the expression for the relaxation rate is

$$\Gamma_{ak} \sim n_a \sigma \delta v \mathcal{N}, \tag{34}$$

where σ is the $\phi + \phi \rightarrow \phi + \phi$ scattering cross-section, and δv represents the velocity dispersion in the fluid. The $\phi + \phi \rightarrow \phi + \phi$ scattering cross-section from the $\lambda\phi^4$ self-interaction is

$$\sigma_\lambda = \frac{\lambda^2}{64\pi} \frac{1}{m_a^2}, \quad (35)$$

whilst the $\phi + \phi \rightarrow \phi + \phi$ scattering cross-section from gravitational interactions is

$$\sigma_g \simeq \frac{4G^2 m_a^2}{(\delta v)^4}. \quad (36)$$

Putting Eqs.35 and 36 into Eq.34, we get the relaxation rate from $\lambda\phi^4$ self-interactions:

$$\Gamma_{a\lambda-k} \sim \frac{\lambda^2}{64\pi} \frac{1}{m_a^2} n_a \delta v \mathcal{N}, \quad (37)$$

the relaxation rate from gravitational interactions:

$$\Gamma_{ag-k} \sim \frac{4G^2 m_a^2}{(\delta v)^4} n_a \delta v \mathcal{N}. \quad (38)$$

• The condensed regime

In this case, the rate at which the occupation number of a typical system oscillator changes is much bigger than the energy exchanged in the transitions it makes. That is, a huge number N of particles occupy a small number K of states, $\mathcal{N} = \frac{N}{K} \gg 1$.

Using Eq. (25), the estimate for the relaxation rate from $\lambda\phi^4$ self-interactions in the condensed regime is [25]

$$\Gamma_{a\lambda-c} \sim \frac{1}{4} n_a \lambda m_a^{-2}, \quad (39)$$

where $n_a = N_a/V$ is the density of particles in the highly occupied, closely spaced states.

Likewise, using Eq. (27), the corresponding relaxation rate from gravitational interactions is

$$\Gamma_{ag-c} \sim 4\pi G n_a m_a^2 \ell_a^2, \quad (40)$$

where $\ell_a \sim 1/p_{\max}$ is the correlation length of the particles.

Relaxation rates with other species

Motivated by the question of whether other species, such as hot particles, photons and other cold species, can come into thermal contact with the cold axion fluid, and thus to explore more cosmic phenomenologies, it is important, especially for the following discussion, to construct the gravitational interaction rates of the cold axion fluid with these other species.

The Hamiltonian describing gravitational interactions between the cold axions and any other species is generally given as

$$H = \sum_{i=1}^M \omega_i a_i^\dagger a_i + \sum_{j=1}^S \omega_j b_j^\dagger b_j + \sum_{i,j,k,l} \frac{1}{4} \Lambda_{kl}^{ij} a_k^\dagger a_l^\dagger a_i a_j + \sum_{i,j,r,s} \Lambda_{b\ js}^{ir} a_j^\dagger b_s^\dagger a_i b_r, \quad (41)$$

where $\Lambda_{b\ js}^{ir} = \left(\Lambda_{b\ ir}^{js}\right)^*$. The b_j^\dagger , b_j , b_r^\dagger , b_r , b_s^\dagger , b_s are the creation and annihilation operators for quanta of the new species, which satisfy canonical (anti)commutation relations. The ω_j are the energies of those quanta. The other symbols (ω_i , a_i and Λ_{kl}^{ij}) have the same meaning as in Eq. (28).

As described before, the same quantization scheme is used with a box of volume $V = L^3$ and periodic boundary conditions. The new particle states are then labeled as $r = (\vec{n}, \sigma)$, with momenta $\vec{p}_b = \frac{2\pi}{L}\vec{n}$, spin σ , and energy $\omega = \sqrt{\vec{p}_b \cdot \vec{p}_b + m_b^2}$, where m_b is the mass of the new species.

The relaxation rate of the new species is then

$$\Gamma_b \sim \lambda_b N \frac{\delta p}{\Delta p_b} \sim \lambda_b N \frac{1}{\ell \Delta p_b}, \quad (42)$$

where $N = K\mathcal{N}$ is the number of cold axions in a volume V , $\delta p \sim 1/\ell$ is the momentum dispersion of cold axions, and Δp_b is the momentum dispersion of the new species⁸. If the new species are degenerate fermions their relaxation rate will be suppressed by Pauli blocking, and thus Eq. (42) only makes sense when the b particles are bosons or non-degenerate fermions.

- Hot particles

The relaxation rate for relativistic particles, e.g. hot axions and non-degenerate neutrinos, interacting with the highly occupied low momentum axion modes is thus of order

$$\Gamma_r \sim 4\pi G n m \ell. \quad (43)$$

- Cold particles

For non-relativistic cold particles, such as hydrogen atoms, baryons/leptons and WIMPs (bosons or non-degenerate fermions), the relaxation rate is

$$\Gamma_B \sim 4\pi G n m \ell \frac{m_B}{\Delta p_B}, \quad (44)$$

where Δp_B is their momentum dispersion.

- Photons

The relaxation rate for photons is

$$\Gamma_\gamma \sim 4\pi G n m \ell, \quad (45)$$

which is the same as for hot particles, Eq. (43), in order of magnitude.

Thermalization rates

Axions are in thermal equilibrium if their relaxation rate Γ_a is large compared to the Hubble expansion rate H . For convenience, we define axion self thermalization rate as: $\frac{\Gamma_a}{H}$. We have noted that the formulae for the relaxation rate differ dependent on the regimes of the axion fluid ('particle kinetic' or 'condensed'). Using Eq. (37) in the particle kinetic regime, we get the axion (and generic ALPs) self thermalization rate due to the self-interaction $\lambda\phi^4$:

$$\frac{\Gamma_{a\lambda.k}}{H} \propto \frac{n_a}{H m_a^2} \propto a(t)^{-3} t \propto t^{-\frac{1}{2}}, \quad (46)$$

where n_a is the axion number density, m_a is the axion mass, $a(t)$ is the cosmic scale factor.

So there must exist a time t_1 , before which the axions thermalize via these self-interactions

$$\Gamma_{a\lambda.k}(t_1) \sim H(t_1), \quad (47)$$

and after which, the axions will fall out of thermal equilibrium.

However, although around t_1 gravitational self-interactions are too weak to cause thermalization of cold axions, after t_1 , the thermalization rate due to gravitational interactions is given by [25, 116]

$$\frac{\Gamma_{ag-c}}{H} \sim \frac{4\pi G n_a m_a^2 \ell_a^2}{H} \propto \frac{a(t_1)}{a(t)} \frac{t}{t_1} \propto a(t). \quad (48)$$

This scales as $a(t)$, and is thus an increasing function of time.

As a consequence, the $\lambda\phi^4$ interaction is only effective at thermalizing axions for a short period in the early Universe, whereas gravitational self-interactions can in contrast be effective at thermalizing axions over long time periods, and hence inducing them to form a BEC.

⁸ If the momentum dispersion is very different in the initial and final states, Δp_b is the larger of the two.

Once thermal equilibrium occurs, there can be cooling effects between particle species. The following condition is the criterion for the cooling effects:

$$\frac{\Gamma_{ag-c}}{H} \sim \frac{4\pi G m_a n_a \ell_a \omega}{\Delta p H} \gtrsim 1, \quad (49)$$

where ω and Δp are the energy and momentum dispersion of the particle species in question.

From another point of view, not only the interaction between the axions themselves, but also the gravitational interaction between the axions and any other particles can lead to thermal equilibrium. When the thermal equilibrium is achieved, there is a heating effect on the lower energy particles, and a cooling effect on the higher energy particles. The generalized thermalization rate is defined as $\frac{\Gamma_b}{H}$. Then the following condition is a criteria for thermal equilibrium, cooling and heating effects:

$$\frac{\Gamma_b}{H} \gtrsim 1. \quad (50)$$

Here b can be r , B , γ , and in particular Hydrogen:

$$\frac{\Gamma_H}{H} \gtrsim 1. \quad (51)$$

Some comments

Although there has been some controversy in the literature[117–119] around the effect of interactions between axions and other particle species, beyond the original progenitors of the scenario it has for example been confirmed that an axion BEC can indeed form in Ref. [120]. Some points remain unsettled at present, insofar as in Ref. [120] it is for example argued that the value of the resulting correlation length may be overly reliant on the criterion of homogeneity and hence reduced to be small, whilst in Ref. [116], it is emphasized that a BEC can be inhomogeneous and nonetheless correlated over its whole extent, which can be arbitrarily large.

IV. Hydrogen cooling induced by axion condensation

The phenomenon discussed in the previous section offers the possibility to explain the anomalous EDGES result, with condensed axion dark matter cooling the primordial hydrogen after it decouples from the CMB at $z \sim 200$.

This latter point is essential, as if axion cooling begins whilst the CMB and hydrogen are in thermal equilibrium, the effect on Eq.(2) will be negligible. Of course the onset of cooling must also occur prior to the cosmic dawn, and the effect in total must give the correct EDGES absorption magnitude. As we will see in the following, and perhaps surprisingly, these various requirements can be simultaneously accommodated by an ALP which may also function as the QCD axion. In practice the EDGES observation uniquely selects a small range for m_a , which is compatible with present-day axion phenomenology and can also conceivably be explored at the next generation of axion experiments.

Using the formulae from the previous section, our starting point is the baryon cooling rate at the time of matter-radiation equality,

$$\frac{\Gamma_H}{H} \sim \frac{4\pi G m_a n_a \ell_a m_H}{\Delta p H} \simeq \frac{4\pi G m_a n_a}{H^2} \left(\frac{m_H}{3T_H} \right)^{1/2}, \quad (52)$$

where we have used the approximation $\rho_a \simeq m_a n_a$, which is sufficiently precise at low temperatures. Assuming that we are in the axion condensed phase, we have also identified the axion BEC correlation length $\ell_a \sim 1/H$ (this value is the extreme limit, before the BEC is formed, the correlation length is smaller, $\sim 1/p_{\max}$ [25]). By virtue of the Maxwell-Boltzmann distribution $\Delta p \simeq \sqrt{3m_H T_H}$, and at this temperature we can identify $\omega \simeq m_H$.

Via the Friedmann equation $3H^2 \simeq 8\pi G \rho_{tot}$ we also have

$$\frac{\Gamma_H}{H} \sim \frac{4\pi G m_a n_a}{(8\pi G/3)\rho_{tot}} \left(\frac{m_H}{3T_H} \right)^{1/2} \simeq \left(\frac{m_H}{3T_H} \right)^{1/2} \frac{3\rho_a}{2\rho_{tot}}. \quad (53)$$

At the epoch of matter-radiation equality, $\rho_{tot} \simeq 2\rho_{DM}$, then, we get

$$\left. \frac{\Gamma_H}{H} \right|_{t_{eq}} \sim \left(\frac{m_H}{3T_H} \right)^{1/2} \left. \frac{3\rho_a}{4\rho_{DM}} \right|_{t_{eq}} = \left(\frac{3m_H}{16T_{eq}} \right)^{1/2} \frac{\Omega_a h^2}{\Omega_{DM} h^2}, \quad (54)$$

neglecting the contributions of visible matter and dark energy. $\Omega_a h^2 / \Omega_{DM} h^2$ is the fraction of the cooling-induced ALP density over the total dark matter relic density.

As $m_H \gg T_{eq}$ we evidently need a small (Ω_a / Ω_{DM}) ratio to ensure cooling begins only when $z \in (200, 20)$. To be more precise we note that since $a \propto t^{2/3}$ during matter domination, we have

$$\frac{\Gamma_H}{H} \sim \frac{4\pi G m_a n_a}{H^2} \left(\frac{m_H}{3T_H} \right)^{1/2} \propto \frac{4\pi G m_a N_a}{a^3 (\dot{a}/a)^2} \left(\frac{m_H}{3T_H} \right)^{1/2} \propto 9\pi G m_a N_a \left(\frac{m_H}{3T_H} \right)^{1/2} \propto \left(\frac{1}{T_H} \right)^{1/2}, \quad (55)$$

where N_a is the total axion number, and a is the cosmic scale factor. This means $\Gamma_H/H \propto 1/\sqrt{T_H}$, which implies that after matter-radiation equality,

$$\frac{\Gamma_H}{H} = \frac{\Gamma_H}{H} \Big|_{t_{eq}} \left(\frac{T_{eq}}{T_H} \right)^{1/2} = \left(\frac{3m_H}{16T_{eq}} \right)^{1/2} \frac{\Omega_a h^2}{\Omega_{DM} h^2} \left(\frac{T_{eq}}{T_H} \right)^{1/2} = \left(\frac{3m_H}{16T_H} \right)^{1/2} \frac{\Omega_a h^2}{\Omega_{DM} h^2}, \quad (56)$$

To have the cooling effect, via Eq.(49), we set $\Gamma_H/H = 1$ to yield

$$\begin{aligned} \frac{\Omega_a h^2}{\Omega_{DM} h^2} &= \left(\frac{16T_H}{3m_H} \right)^{1/2}, \\ \Omega_a h^2 &= \left(\frac{16T_H}{3m_H} \right)^{1/2} \Omega_{DM} h^2. \end{aligned} \quad (57)$$

Since $T_{eq} \sim 0.75 \text{ eV} \simeq 8.7 \times 10^3 \text{ K}$, and we require axion-induced cooling to occur between $T_H^{z=200} \sim 475 \text{ K}$ and $T_H^{z=20} \sim 10 \text{ K}$, we can firstly establish the requirement

$$\frac{\Omega_a h^2}{\Omega_{DM} h^2} \in (0.22, 1.5) \times 10^{-5}. \quad (58)$$

It is important to note that once condensation occurs, we will have two distinct populations of cold axions; those that are in the condensed state, and a remnant thermal population. Hydrogen can in principle interact with both, however there exists a key distinction: scattering from the cold thermal axions will simply raise their temperature, whilst scattering condensed axions will typically liberate them from the BEC, given the energies involved, and into the thermal population.

However, in Ref. [119] the rate at which the BEC occupation number can change via scattering with external particles is calculated, finding that the latter number-changing process should be vanishingly rare. To be careful though, this only means that the BEC cannot be excited directly by the hydrogen, and does not exclude that the BEC cannot rethermalize by itself. As such the total BEC axion occupation number density can in principle change.

Since the energy lost from the hydrogen must be transferred to the thermal axions, energy conservation requires

$$\rho_H(T_{Hi}) + \rho_{ac}(T_{ai}) + \rho_{at}(T_{ai}) = \rho_H(T_f) + \rho_{ac}(T_f) + \rho_{at}(T_f). \quad (59)$$

Here, T_{Hi} , T_{ai} are the initial (pre-cooling) hydrogen, BEC axion temperatures, respectively. T_f is the final (post-cooling) temperature of hydrogen and BEC axion. In fact, T_{Hi} is just equal to T_H of the Λ CDM before BEC axion cooling, here for comparing with the T_f , we use T_{Hi} , especially in the following cooling related equations, and always use T_H as the usual hydrogen temperature of Λ CDM. $\rho_H(T_{Hi})$, $\rho_{ac}(T_{ai})$, $\rho_{at}(T_{ai})$ are the initial (pre-cooling) hydrogen, BEC axion, and thermal axion energy densities, respectively. Meanwhile $\rho_H(T_f)$, $\rho_{ac}(T_f)$, $\rho_{at}(T_f)$ are the final (post-cooling) hydrogen, BEC axion, and thermal axion energy densities, respectively.

Because T_{ai} is very low, $\rho_a(T_{ai})$ is small enough to be ignored. So that the conservation equation becomes

$$\rho_H(T_{Hi}) \simeq \rho_H(T_f) + \rho_{at}(T_f) - \rho_{at(\text{rest mass})}, \quad (60)$$

where, $\rho_{at(\text{rest mass})} = \rho_{ac}(T_{ai}) - \rho_{ac}(T_f)$ means the rest mass energy density of the axions entering the thermal axion population from the BEC axion population via rethermalization^{9, 10}.

⁹ This is strictly a slightly more precise energy conservation equation than that used in Ref. [9], although the effect of the additional term on our final result is negligible thanks to the 4th order root extraction.

¹⁰ For our parameter range of interest, both photon cooling by axions and thermal axion heating by photons is strongly suppressed, as there is no large $\sqrt{m_H/(3T_H)}$ factor in the corresponding photon cooling rate, see Eqs.(45), (44), (52). We also note the principal constraint in the axion-induced cooling ${}^7\text{Li}$ scenario was a large resulting N_{eff} at recombination. For us this is not a cause for concern as we are operating at a much later epoch, and the thermal axions excited will be non-relativistic.

In the case of cold hydrogen, to the lowest order, we have

$$\rho_H(T_H) \simeq n_H(m_H + 3T_H/2), \quad (61)$$

where n_H is the Hydrogen number density. Since hydrogen comprises the vast majority of baryonic matter at this epoch we can use the baryon-to-photon ratio to estimate

$$n_H \simeq 6 \times 10^{-10} n_\gamma, \quad (62)$$

where n_γ is the photon number density

$$n_\gamma = 2\zeta(3)T_\gamma^3/\pi^2. \quad (63)$$

For simplicity, we can assume

$$\begin{aligned} T_\gamma &\simeq T_\gamma^{z=200} \times \frac{z+1}{200+1}, \\ T_H &\simeq T_H^{z=200} \times \left(\frac{z+1}{200+1} \right)^2. \end{aligned} \quad (64)$$

Where the formula for T_γ is accurate enough, but the formula for T_H is not so accurate. We provide this formula primarily to illustrate how the final result is computed, in practice we use RECFast to get a more accurate relation in the following sections.

Inserting a Maxwell-Boltzmann distribution for the thermal axion population we have:

- The energy density of thermal axions

$$\rho_{at}(T) = \frac{T^4}{2\pi^2} \int_0^\infty \frac{\xi^2 \sqrt{\xi^2 + (m_a/T)^2}}{\exp\left(\sqrt{\xi^2 + (m_a/T)^2}\right) - 1} d\xi. \quad (65)$$

- The number density of thermal axions

$$n_{at}(T) = \frac{T^3}{2\pi^2} \int_0^\infty \frac{\xi^2}{\exp\left(\sqrt{\xi^2 + (m_a/T)^2}\right) - 1} d\xi. \quad (66)$$

- The rest mass energy density of the rethermalized axions

$$\rho_{at(\text{rest mass})} = (n_{at}(T_f) - n_{at}(T_{ai}))m_a \simeq n_{at}(T_f)m_a = \frac{T_f^3 m_a}{2\pi^2} \int_0^\infty \frac{\xi^2}{\exp\left(\sqrt{\xi^2 + (m_a/T_f)^2}\right) - 1} d\xi. \quad (67)$$

Putting all the Eqs.(61), (65), (67), into eq.(60), we get a complicated expression for the final energy conservation equation, with three unknown variables m_a , T_{Hi} and T_f . If given T_{Hi} and m_a , we can solve this equation numerically for T_f and hence the cooling ratio T_f/T_{Hi} .

By Eq.(64) and assuming the change in z is negligible during the cooling process, we find the cooled Hydrogen temperature at redshift z is

$$T_{Hc} \simeq T_f \left(\frac{z+1}{z_c+1} \right)^2 = T_{Hi} \left(\frac{z+1}{z_c+1} \right)^2 \left(\frac{T_f}{T_{Hi}} \right) = T_H \left(\frac{T_f}{T_{Hi}} \right), \quad (68)$$

where z_c is the redshift at which cooling begins, $z < z_c$, and T_H takes its usual Λ CDM value.

Since $T_s = T_H$ at this epoch, we then find the cooled spin temperature is

$$T_{sc} \simeq T_H \left(\frac{T_f}{T_{Hi}} \right). \quad (69)$$

Putting this result into Eq.(2), we arrive at

$$T_{21} = 35 \text{ mK} \left(1 - \frac{T_{Hi}}{T_f} \frac{T_\gamma}{T_H} \right) \sqrt{\frac{1+z}{18}}, \quad (70)$$

where T_γ and T_H take their usual Λ CDM values.

From the EDGES result, T_{21} is limited in a range:

$$T_{21}^{z \sim 17} \in (-0.94, -0.34) \text{ K} \quad (71)$$

This limit condition will give some important constraints on the axion parameter space, which will be illustrated in the following section.

For a brief overview of the cooling process, we offer the following schematic graph:

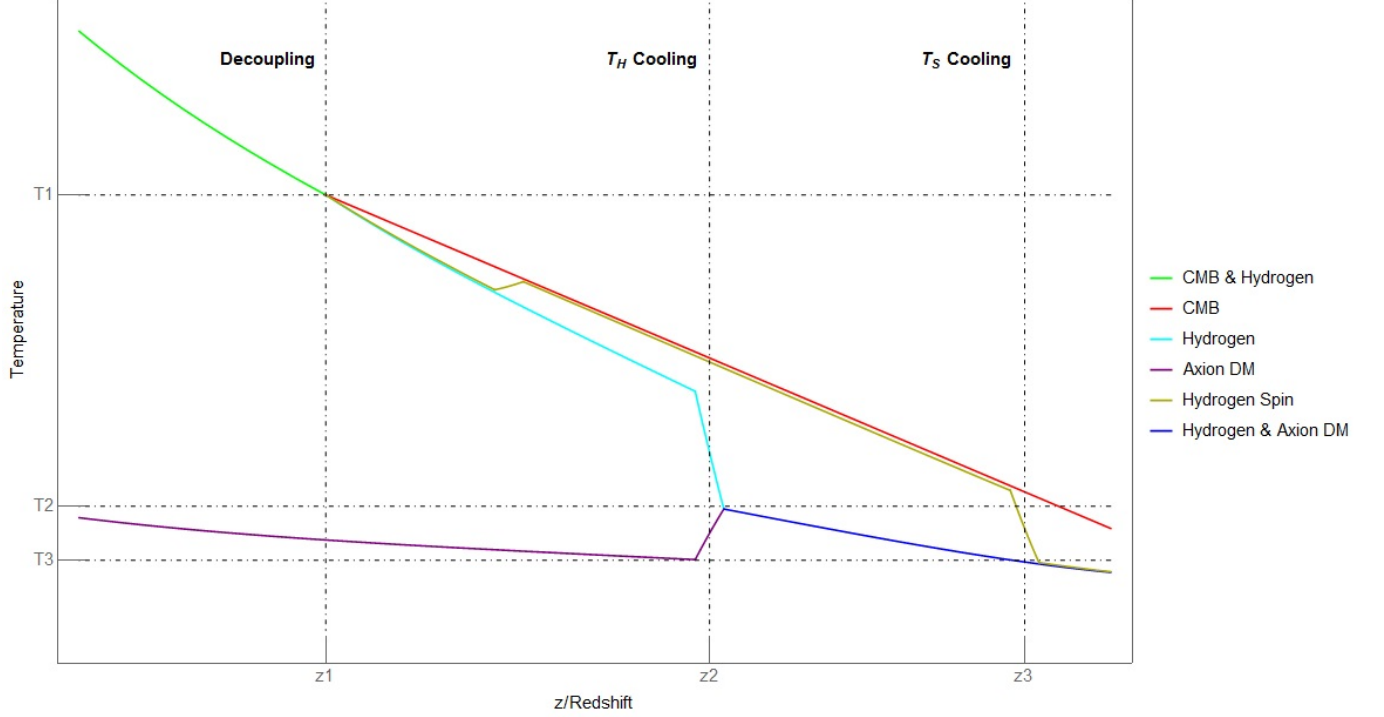


FIG. 1. Schematic overview of the axion-hydrogen cooling process. Here z_1 is the redshift when hydrogen and the CMB decoupled at the temperature T_1 ; z_2 is the redshift when hydrogen was cooled by the axion dark matter to the temperature T_2 ; and z_3 is the redshift when the hydrogen spin temperature was coupled to the hydrogen temperature via the Wouthuysen-Field effect and so reduced to the temperature T_3 .

V. Numerical computation and experimental constraints

Based on the previous derivations and formulae, we can then now calculate our desired result. In practice additional care is needed since the basic redshift relations do not accurately capture the evolution of T_H in this region, so we use RECFAST to compute T_H and T_γ [121]. Numerically fitting we find

$$T_H = \frac{0.267628 + 0.0034228z + 0.0241129z^2 - 0.0000872526z^3 + 1.30977 \times 10^{-7}z^4 - 3.33753 \times 10^{-11}z^5}{11605},$$

$$T_\gamma = \frac{2.725 + 2.725z - 1.05 \times 10^{-18}z^2}{11605}, \quad (72)$$

as shown in Figure 2.

We can find CMB temperature is almost linear with redshift z , while hydrogen gas temperature is more complicated, and in fact the decoupling of the CMB and hydrogen gas begins earlier than $z = 200$. The new accurate fitting relation of T_H and z is the basic reason of the numerical differences between the present paper and our previous short paper [9].

The resulting dependence in Eq.(70) is however nonetheless correct, and so we can use Eq.(60) to find the resulting 21 cm absorption feature.

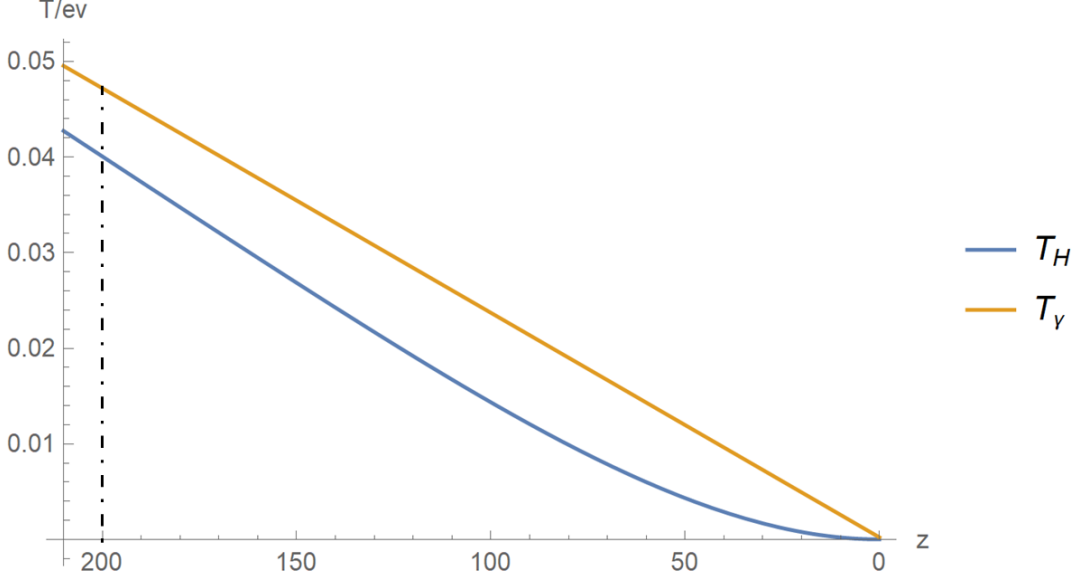


FIG. 2. The temperature evolution of Hydrogen gas and the CMB.

V.A. The mass and relic density constraint

The energy conservation equation Eq.(60) has three unknown variables m_a , T_{Hi} , T_f . Here T_{Hi} is determined by z_c . For practical computation we construct an array of values for z_c and $x = m_a/T_f$ respectively, then for every pair of (z_c, x) , solve for the value of m_a , and hence $T_f = m_a/x$. So, for a certain value m_a , there are many different (z_c, x) or (T_{Hi}, T_f) pair values. Equivalently, by equation Eq.(57), $\Omega_a h^2$ is determined by T_{Hi} , so we can also say for a certain value m_a there are many different possible $(\Omega_a h^2, T_f)$ values.

From Eq.(70), we can find T_{21} in terms of two independent variables, m_a and $\Omega_a h^2$. From the ranges given by (71) and (58), we can then get a constraint on m_a and $\Omega_a h^2$ as given in Fig. 3. By virtue of the EDGES best-fit result, where each value gives $T_{21} \simeq -0.52$ K at $z \sim 17$, we will favour an ALP with mass $m_a \in (6, 400)$ meV. If we relax $T_{21} \in (-0.94, -0.34)$ K at $z \sim 17$ ¹¹, the 99% confidence limits presented in Eq.(2), ALP mass will get a bigger range of $m_a \in (2.7, 640)$ meV.

Since in the generic ALP case the relationship between $\Omega_a h^2$ and m_a is unfixed, we cannot directly connect them to coupling constraints and thus standard axion phenomenology. However, for the QCD axion the corresponding f_a is given via

$$\Omega_a h^2 = 0.15X \left(\frac{f_a}{10^{12} \text{ GeV}} \right)^{7/6}, \quad (73)$$

where X is scenario-dependent unknown parameter. For PQ symmetry breaking prior to inflation typically $X \simeq \sin^2 \theta_{mis}/2$, whilst for PQ symmetry breaking after inflation typically $X \in (2, 10)$ depending on the relative contributions of topological defect decays and vacuum misalignment [26]. Combing these two scenarios, generally we have $X \in (0, 10)$. By Eq.(58), this implies that

$$f_a \in (1.2, 6.1) \times X^{-6/7} \times 10^7 \text{ GeV}, \quad (74)$$

which is in turn related through chiral perturbation theory to m_a via

$$m_a \simeq 6 \text{ eV} \left(\frac{10^6 \text{ GeV}}{f_a} \right), \quad (75)$$

¹¹ Here we remind the reader that $T_{21} \simeq -0.21$ K is the standard Λ CDM result, which we reach in the limit of this mechanism being inoperative.

yielding

$$m_a \simeq 1.18 \times 10^{-6} \text{ eV} \left(\frac{\Omega_a h^2}{X} \right)^{-6/7}, \quad (76)$$

where care is required in that m_a is now not freely varied in this instance; each value is associated to a specific $\Omega_a h^2$, and thus the specific z_c and T_{Hi} at which cooling begins. Additionally by Eq.(58), numerically, we get

$$m_a \in (0.1, 0.5) \times X^{6/7} \text{ eV}. \quad (77)$$

Taking care to accommodate this, we arrive at a one-to-one mapping between m_a and T_{21} . We also note for completeness that in this mass range we can expect both hot and cold axion dark matter, due, for example, to thermal production and vacuum misalignment respectively.

Since $X \in (2, 10)$ for post-inflationary PQ symmetry breaking, the minimum value for this quantity is realized for pre-inflationary symmetry breaking, in which case we have $X^{6/7} \sim 0.5$ in the absence of fine-tuning, assuming the initial misalignment angle is randomly drawn from a uniform distribution on $[-\pi, \pi]$, giving $\langle \theta_{\text{mis}}^2 \rangle = \pi^2/3$.

Varying X we will find a preferred natural range of $m_a \in (6, 400)$ meV for the QCD axion by virtue of the EDGES best-fit result (where each value gives $T_{21} \simeq -0.52$ K at $z \sim 17$ as mentioned before), this is same with the ALP situation.

If we fix $X^{6/7} = 1$ as a benchmark case and relax $T_{21} \in (-0.94, -0.34)$ K at $z \sim 17$, working backwards, then in this case imply $m_a \in (120, 170)$ meV, with the best fit value corresponding to $m_a \simeq 150$ meV. For more $X^{6/7}$ benchmark values, see the following table.

$X^{6/7}$ benchmark	min mass (/meV)	best fit mass (/meV)	max mass (/meV)
1	120	150	170
0.5	73	90	100
0.1	23	28	33

TABLE I. The QCD axion mass range for several $X^{6/7}$ benchmark values.

Considering all these ALP and QCD axion possibilities, we show the parameter space in Fig. 3, where the QCD axion is represented via lines of constant $X^{6/7}$.

V.B. The mass and coupling constraint

Since the generic ALP case does not immediately translate to ordinary axion coupling constant constraints, we can specialize to the QCD axion to gain some phenomenological insight and delineate the parameter values implied by the EDGES observation in this scenario, along with the various experimental and observational constraints which may apply. In Fig. 4 we reproduce constraints on the axion parameter space in our region of interest from [134] colour coded with the resulting value of T_{21} at $z = 17$ for the benchmark case of $X = 1$ (That is $m_a \in (120, 170)$ meV). As is evident, the EDGES observations can be straightforwardly accommodated within the ordinary QCD axion band.

It is of course important to note that the full possible mass range favoured by these results is strongly disfavoured for DFSZ type axions due to stellar energy-loss constraints [70, 71, 122]. As such we are implicitly considering KSVZ type axions [68, 69], although the ratio E/N of the electromagnetic to colour anomaly is however allowed to vary within the usual range to accommodate variant models of the QCD axion [75, 76].

Strictly speaking even then there is some tension between our preferred mass range and the observed burst duration of SN1987A, which favours $f_a \gtrsim 4 \times 10^8$ GeV for standard QCD axions [123]. This arises from an inference of the SN1987A cooling timescale, and thus energy loss to axions, from the time interval between the first and last neutrino observation. However, given that these limits are derived from a single observation, and not to mention our limited knowledge regarding about axion emission in this extreme environment (the resulting exclusion being ‘fraught with uncertainties’ in the words of Ref. [123]), we can follow the example of others (e.g. Ref. [124]) and exercise a measure of caution in applying this constraint.

Furthermore, in Ref. [126], the top two panels of Figure 2 suggest that the mass range in question can still be compatible with DFSZ axions in a region favored by stars, and furthermore in fact seems to be particularly interesting for DFSZ-II models. We also notice that in a recent preprint [127] the author argues that those bounds are actually overestimated by an order of magnitude and recalculates to find weaker constraints, which would then marginally

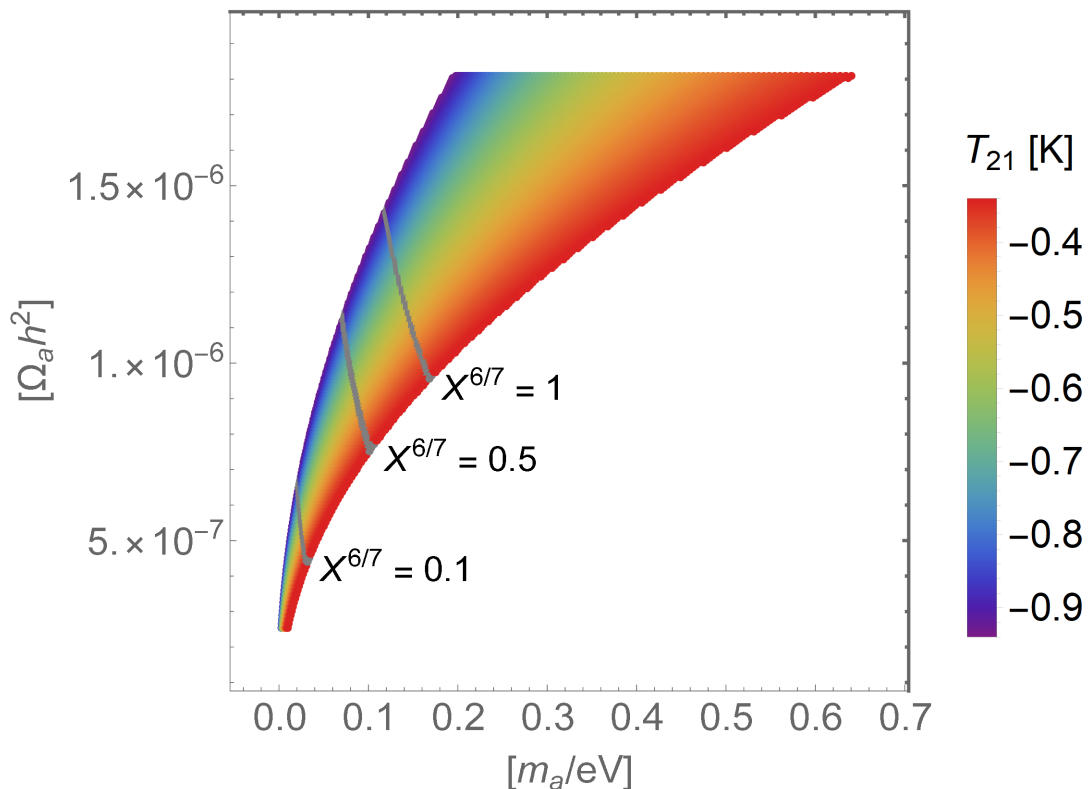


FIG. 3. The ALP ($m_a, \Omega_a h^2$) parameter space satisfying Eq.(58), colour-coded with the resulting 21cm brightness temperature at $z = 17$. Comparison with the best-fit EDGES result suggests a $m_a \in (6, 400)$ meV range of compatibility. Since the QCD axion fixes the relationship between these quantities in terms of the dark matter density parameter X appearing in Eq.(73), we overlay lines of fixed X to show dependence on this quantity.

permit e.g. DFSZ axions in our 21 cm scenario. So-called ‘astrophobic’ axion models are also noteworthy here, where $\mathcal{O}(100)$ meV axion masses are allowed at the cost of introducing some flavour-violating couplings [77, 128].

In addition, we can also recapitulate at this point that ultimately the axion cooling mechanism employed here is gravitationally mediated, and so could be achieved with no Standard Model couplings whatsoever, and thus no issues in this regard. By extension, the use of the QCD axion is in this context non-essential, and our primary results for generic axion-like-particles can still apply regardless.

We can also note from Ref. [124] that although our mass range of interest evades hot dark matter constraints at present, future large scale surveys such as the EUCLID mission are in conjunction with Planck CMB data projected to probe $m_a \gtrsim 150$ meV for the QCD axion at high significance, allowing this scenario to be definitively tested in the near future [125]. More specifically, EUCLID will probe at the expansion of the universe and large scale structure, via galaxy observations out to $z \sim 2$. Axions can be produced thermally if their couplings are not extremely suppressed, and so act as hot dark matter, which has a very different phenomenology compared to cold dark matter. Once the mass of QCD axion is above 150 meV, it will have couplings strong enough that it can be copiously produced via thermal processes during the QCD phase transition, resulting in too much hot dark matter, which alters structure formation in a way detectable by EUCLID.

Inspired from Ref. [10], we note that our mechanism may have a damping effect on Baryon Acoustic Oscillations (BAO). Although it is ultimately argued there that the net effect on BAO should be consistent with observations, it may be worthwhile to more deeply explore the consequences of this scenario for this and other cosmological observables. As such BAO related experiments, such as eBOSS [129, 130], may also be of relevance to this scenario.

VI. Summary

The EDGES collaboration have recently presented an anomalously strong 21cm absorption profile, which could be the result of dark matter interactions around the time of the cosmic dawn. Despite a flurry of interest there is as of

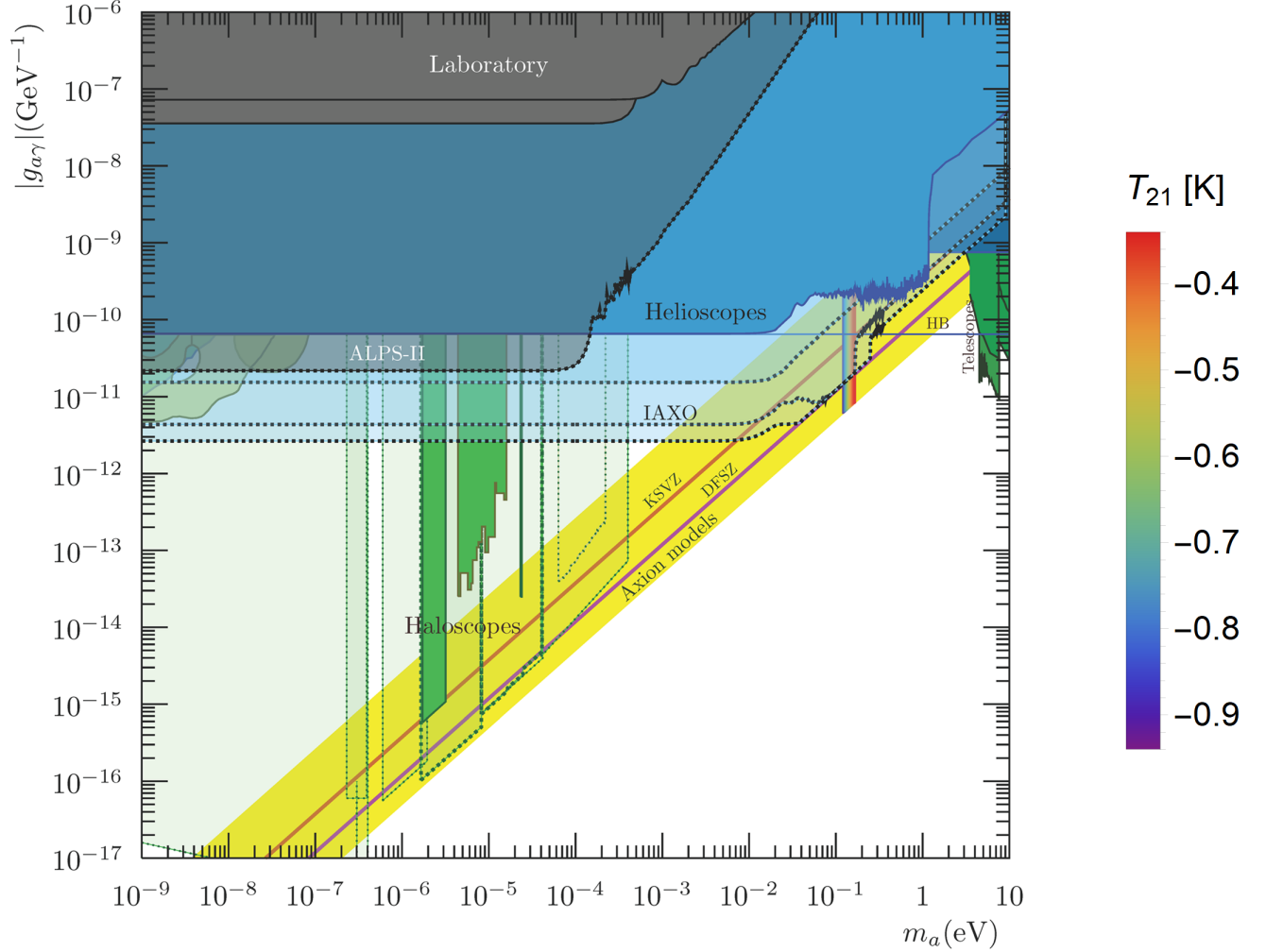


FIG. 4. The region of the axion parameter space relevant for our purposes, reproduced from [134], with the 21cm brightness temperature at $z \sim 17$ overlaid from axion-induced cooling processes in the benchmark case of $X = 1$. The yellow band denotes QCD axion models with varying electromagnetic/colour anomaly coefficients, whilst the black curves indicate forecast sensitivities for the proposed IAXO experiment. The best fit m_a value preferred by the EDGES observations in this case is 150 meV.

yet no clear consensus on the provenance of this effect, and whether it is indeed a signature of dark matter at all. However, these results nonetheless provide an exciting first window into a previously unexplored epoch.

We have in this paper explored the potential of condensed-phase axion dark matter to explain these anomalous observations via a reduction of the hydrogen spin temperature during this epoch. By fixing the axion CDM relic density so that cooling begins within the appropriate epoch, we find cooling effects that are both capable of explaining the EDGES observations and compatible with present day axion phenomenology. More specifically, we find that the EDGES best-fit result of $T_{21} \simeq -0.52$ K and the requirement that hydrogen cooling occur within the range $z \in (200, 20)$ are consistent with the cooling induced by an axion-like-particle of mass $m_a \in (6, 400)$ meV. Future experiments and large scale surveys, particularly the International Axion Observatory (IAXO) and EUCLID, should have the capability to directly test this scenario.

As however the underlying cooling mechanism relies only upon gravitational couplings, it is not limited strictly to the context of models of the QCD axion. As such it may also be arranged to occur in the primary scenario of axion-like-particles with no Standard Model couplings whatsoever, which could then evade bounds from stellar cooling

and supernova observations.

Acknowledgments

This research was supported by Scientific Research Starting Project for Advanced Imported Talents of Wuyi University, by a CAS President's International Fellowship, by the Projects 11875062, 11947302 and 11875148 supported by the National Natural Science Foundation of China, and by the Key Research Program of Frontier Science, CAS. The numerical results described in this paper have been obtained via the HPC Cluster of ITP-CAS, Beijing, China.

-
- [1] J. D. Bowman, A. E. E. Rogers, R. A. Monsalve, T. J. Mozdzen and N. Mahesh, *Nature* **555** (2018) no.7694, 67.
 - [2] R. Barkana, *Nature* **555** (2018) no.7694, 71 [arXiv:1803.06698 [astro-ph.CO]].
 - [3] J. B. Munoz and A. Loeb, arXiv:1802.10094 [astro-ph.CO].
 - [4] A. Berlin, D. Hooper, G. Krnjaic and S. D. McDermott, arXiv:1803.02804 [hep-ph].
 - [5] R. Barkana, N. J. Outmezguine, D. Redigolo and T. Volansky, arXiv:1803.03091 [hep-ph].
 - [6] A. A. Costa, R. C. G. Landim, B. Wang and E. Abdalla, arXiv:1803.06944 [astro-ph.CO].
 - [7] C. Li and Y. F. Cai, arXiv:1804.04816 [astro-ph.CO].
 - [8] G. Lambiase and S. Mohanty, arXiv:1804.05318 [hep-ph].
 - [9] N. Houston, C. Li, T. Li, Q. Yang and X. Zhang, arXiv:1805.04426 [hep-ph].
 - [10] P. Sikivie, arXiv:1805.05577 [astro-ph.CO].
 - [11] J. C. Hill and E. J. Baxter, arXiv:1803.07555 [astro-ph.CO].
 - [12] T. R. Slatyer and C. L. Wu, *Phys. Rev. D* **98**, no. 2, 023013 (2018) doi:10.1103/PhysRevD.98.023013 [arXiv:1803.09734 [astro-ph.CO]].
 - [13] A. Falkowski and K. Petraki, arXiv:1803.10096 [hep-ph].
 - [14] C. Feng and G. Holder, *Astrophys. J.* **858**, no. 2, L17 (2018) doi:10.3847/2041-8213/aac0fe [arXiv:1802.07432 [astro-ph.CO]].
 - [15] A. Ewall-Wice, T. C. Chang, J. Lazio, O. Dore, M. Seiffert and R. A. Monsalve, arXiv:1803.01815 [astro-ph.CO].
 - [16] S. Fraser *et al.*, arXiv:1803.03245 [hep-ph].
 - [17] M. Pospelov, J. Pradler, J. T. Ruderman and A. Urbano, *Phys. Rev. Lett.* **121**, no. 3, 031103 (2018) doi:10.1103/PhysRevLett.121.031103 [arXiv:1803.07048 [hep-ph]].
 - [18] K. Lawson and A. R. Zhitnitsky, arXiv:1804.07340 [hep-ph].
 - [19] T. Moroi, K. Nakayama and Y. Tang, arXiv:1804.10378 [hep-ph].
 - [20] D. Aristizabal Sierra and C. S. Fong, *Phys. Lett. B* **784**, 130 (2018) doi:10.1016/j.physletb.2018.07.047 [arXiv:1805.02685 [hep-ph]].
 - [21] Y. Wang and G. B. Zhao, arXiv:1805.11210 [astro-ph.CO].
 - [22] L. F. Xiao, R. An, L. Zhang, B. Yue, Y. Xu and B. Wang, arXiv:1807.05541 [astro-ph.CO].
 - [23] R. Hills, G. Kulkarni, P. D. Meerburg and E. Puchwein, arXiv:1805.01421 [astro-ph.CO].
 - [24] Y. Xu, B. Yue and X. Chen, arXiv:1806.06080 [astro-ph.CO].
 - [25] P. Sikivie and Q. Yang, *Phys. Rev. Lett.* **103** (2009) 111301 [arXiv:0901.1106 [hep-ph]].
 - [26] O. Erken, P. Sikivie, H. Tam and Q. Yang, *Phys. Rev. D* **85** (2012) 063520 [arXiv:1111.1157 [astro-ph.CO]].
 - [27] O. Erken, P. Sikivie, H. Tam and Q. Yang, *Phys. Rev. Lett.* **108** (2012) 061304 [arXiv:1104.4507 [astro-ph.CO]].
 - [28] E. Armengaud *et al.*, *JINST* **9** (2014) T05002 [arXiv:1401.3233 [physics.ins-det]].
 - [29] R. Laureijs *et al.* [EUCLID Collaboration], arXiv:1110.3193 [astro-ph.CO].
 - [30] P. Madau, A. Meiksin and M. J. Rees, *Astrophys. J.* **475**, 429 (1997) doi:10.1086/303549 [astro-ph/9608010].
 - [31] J. R. Pritchard and A. Loeb, *Rept. Prog. Phys.* **75**, 086901 (2012) doi:10.1088/0034-4885/75/8/086901 [arXiv:1109.6012 [astro-ph.CO]].
 - [32] S. A. Wouthuysen. On the excitation mechanism of the 21-cm (radio-frequency) interstellar hydrogen emission line. *AJ*, 57:31, 1952.
 - [33] G. B. Field. Excitation of the Hydrogen 21cm line. *Proc. I. R. E.*, 46:240, 1958.
 - [34] J. Mirocha, G. J. A. Harker and J. O. Burns, *Astrophys. J.* **777**, 118 (2013) doi:10.1088/0004-637X/777/2/118 [arXiv:1309.2296 [astro-ph.CO]].
 - [35] J. Mirocha, G. J. A. Harker and J. O. Burns, *Astrophys. J.* **813**, no. 1, 11 (2015) doi:10.1088/0004-637X/813/1/11 [arXiv:1509.07868 [astro-ph.CO]].
 - [36] J. Mirocha, R. H. Mebane, S. R. Furlanetto, K. Singal and D. Trinh, *Mon. Not. Roy. Astron. Soc.* **478**, no. 4, 5591 (2018) doi:10.1093/mnras/sty1388 [arXiv:1710.02530 [astro-ph.GA]].
 - [37] Swarup, G. 1990, *Indian Journal of Radio and Space Physics*, 19, 493
 - [38] Swarup, G. 1991, *IAU Colloq. 131: Radio Interferometry. Theory, Techniques, and Applications*, 19, 376
 - [39] U. L. Pen, X. P. Wu and J. Peterson, [astro-ph/0404083].

- [40] A. Lidz, O. Zahn, M. McQuinn, M. Zaldarriaga and L. Hernquist, *Astrophys. J.* **680**, 962 (2008) doi:10.1086/587618 [arXiv:0711.4373 [astro-ph]].
- [41] C. J. Lonsdale *et al.*, *IEEE Proc.* **97**, 1497 (2009) doi:10.1109/JPROC.2009.2017564 [arXiv:0903.1828 [astro-ph.IM]].
- [42] M. P. van Haarlem *et al.*, *Astron. Astrophys.* **556**, A2 (2013) doi:10.1051/0004-6361/201220873 [arXiv:1305.3550 [astro-ph.IM]].
- [43] Bradley, R., Backer, D., Parsons, A., Parashare, C., & Gugliucci, N. E. 2005, *Bulletin of the American Astronomical Society*, **37**, 33.01
- [44] R. Braun, *Astrophys. Space Sci. Libr.* **207**, 167 (1996) doi:10.1007/978-94-009-1734-7_10 [astro-ph/9512060].
- [45] C. L. Carilli and S. Rawlings, *New Astron. Rev.* **48**, 979 (2004) doi:10.1016/j.newar.2004.09.001 [astro-ph/0409274].
- [46] N. Kanekar and F. H. Briggs, *New Astron. Rev.* **48**, 1259 (2004) doi:10.1016/j.newar.2004.09.030 [astro-ph/0409169].
- [47] Schilizzi, R. T. 2004, *procspie*, 5489, 62
- [48] L. Feretti, *Frascati Phys. Ser.* **64**, 283 (2017).
- [49] P. Bull *et al.*, arXiv:1810.02680 [astro-ph.CO].
- [50] T. C. Voytek, A. Natarajan, J. M. Jáuregui García, J. B. Peterson and O. López-Cruz, *Astrophys. J.* **782**, L9 (2014) doi:10.1088/2041-8205/782/1/L9 [arXiv:1311.0014 [astro-ph.CO]].
- [51] L. J. Greenhill and G. Bernardi, arXiv:1201.1700 [astro-ph.CO].
- [52] S. Singh *et al.*, *Astrophys. J.* **845**, no. 2, L12 (2017) doi:10.3847/2041-8213/aa831b [arXiv:1703.06647 [astro-ph.CO]].
- [53] G. De Zotti *et al.* [CORE Collaboration], *JCAP* **1804**, no. 04, 020 (2018) doi:10.1088/1475-7516/2018/04/020 [arXiv:1609.07263 [astro-ph.GA]].
- E. Di Valentino *et al.* [CORE Collaboration], *JCAP* **1804**, 017 (2018) doi:10.1088/1475-7516/2018/04/017 [arXiv:1612.00021 [astro-ph.CO]].
- F. Finelli *et al.* [CORE Collaboration], *JCAP* **1804**, 016 (2018) doi:10.1088/1475-7516/2018/04/016 [arXiv:1612.08270 [astro-ph.CO]].
- J. B. Melin *et al.* [CORE Collaboration], *JCAP* **1804**, no. 04, 019 (2018) doi:10.1088/1475-7516/2018/04/019 [arXiv:1703.10456 [astro-ph.CO]].
- M. Remazeilles *et al.* [CORE Collaboration], *JCAP* **1804**, no. 04, 023 (2018) doi:10.1088/1475-7516/2018/04/023 [arXiv:1704.04501 [astro-ph.CO]].
- C. Burigana *et al.* [CORE Collaboration], *JCAP* **1804**, no. 04, 021 (2018) doi:10.1088/1475-7516/2018/04/021 [arXiv:1704.05764 [astro-ph.CO]].
- P. de Bernardis *et al.* [CORE Collaboration], *JCAP* **1804**, no. 04, 015 (2018) doi:10.1088/1475-7516/2018/04/015 [arXiv:1705.02170 [astro-ph.IM]].
- J. Delabrouille *et al.* [CORE Collaboration], *JCAP* **1804**, no. 04, 014 (2018) doi:10.1088/1475-7516/2018/04/014 [arXiv:1706.04516 [astro-ph.IM]].
- A. Challinor *et al.* [CORE Collaboration], *JCAP* **1804**, no. 04, 018 (2018) doi:10.1088/1475-7516/2018/04/018 [arXiv:1707.02259 [astro-ph.CO]].
- P. Natoli *et al.* [CORE Collaboration], *JCAP* **1804**, no. 04, 022 (2018) doi:10.1088/1475-7516/2018/04/022 [arXiv:1707.04224 [astro-ph.CO]].
- [54] Philip, L., Abdurashidova, Z., Chiang, H. C., et al. 2018, arXiv:1806.09531
- [55] Mozdzen, T. J., Bowman, J. D., Monsalve, R. A., & Rogers, A. E. E. 2016, *mnras*, 455, 3890
- [56] A. E. E. Rogers J. D. Bowman J. Vierinen R. Monsalve T. Mozdzen 10 January 2015 <https://doi.org/10.1002/2014RS005599>
- [57] R. A. Monsalve, A. E. E. Rogers, J. D. Bowman and T. J. Mozdzen, *Astrophys. J.* **835**, no. 1, 49 (2017) doi:10.3847/1538-4357/835/1/49 [arXiv:1602.08065 [astro-ph.IM]].
- [58] R. Hills, G. Kulkarni, P. D. Meerburg & E. Puchwein, *Nature* **564**, no. 7736, E32 (2018) doi:10.1038/s41586-018-0796-5 [arXiv:1805.01421 [astro-ph.CO]].
- [59] Judd D. Bowman, Alan E. E. Rogers, Raul A. Monsalve, Thomas J. Mozdzen & Nivedita Mahesh *Nature* **564**, E35 (2018) doi:10.1038/s41586-018-0797-4
- [60] Mesinger, A., Furlanetto, S., & Cen, R. 2011, *mnras*, 411, 955
- [61] Cohen, A., Fialkov, A., Barkana, R., & Lotem, M. 2017, *mnras*, 472, 1915
- [62] D. J. E. Marsh, *Phys. Rept.* **643**, 1 (2016) doi:10.1016/j.physrep.2016.06.005 [arXiv:1510.07633 [astro-ph.CO]].
- [63] Q. Yang, *Mod. Phys. Lett. A* **32**, 1740003 (2017) doi:10.1142/S021773231740003X [arXiv:1509.00673 [hep-ph]].
- [64] J. E. Kim, *PoS CORFU* **2016**, 037 (2017) doi:10.22323/1.292.0037 [arXiv:1703.03114 [hep-ph]].
- [65] R. D. Peccei and H. R. Quinn, *Phys. Rev. Lett.* **38** (1977) 1440. doi:10.1103/PhysRevLett.38.1440
- [66] S. Weinberg, *Phys. Rev. Lett.* **40** (1978) 223. doi:10.1103/PhysRevLett.40.223
- [67] F. Wilczek, *Phys. Rev. Lett.* **40** (1978) 279. doi:10.1103/PhysRevLett.40.279
- [68] J. E. Kim, *Phys. Rev. Lett.* **43** (1979) 103. doi:10.1103/PhysRevLett.43.103
- [69] M. A. Shifman, A. I. Vainshtein and V. I. Zakharov, *Nucl. Phys. B* **166** (1980) 493. doi:10.1016/0550-3213(80)90209-6
- [70] M. Dine, W. Fischler and M. Srednicki, *Phys. Lett.* **104B** (1981) 199. doi:10.1016/0370-2693(81)90590-6
- [71] A. R. Zhitnitsky, *Sov. J. Nucl. Phys.* **31** (1980) 260 [*Yad. Fiz.* **31** (1980) 497].
- [72] R. J. Crewther, P. Di Vecchia, G. Veneziano and E. Witten, *Phys. Lett.* **88B**, 123 (1979) Erratum: [*Phys. Lett.* **91B**, 487 (1980)]. doi:10.1016/0370-2693(80)91025-4, 10.1016/0370-2693(79)90128-X
- [73] C. A. Baker *et al.*, *Phys. Rev. Lett.* **97**, 131801 (2006) doi:10.1103/PhysRevLett.97.131801 [hep-ex/0602020].
- [74] C. Vafa and E. Witten, *Phys. Rev. Lett.* **53**, 535 (1984). doi:10.1103/PhysRevLett.53.535
- [75] L. Di Luzio, F. Mescia and E. Nardi, *Phys. Rev. Lett.* **118** (2017) no.3, 031801 [arXiv:1610.07593 [hep-ph]].

- [76] L. Di Luzio, F. Mescia and E. Nardi, Phys. Rev. D **96** (2017) no.7, 075003 [arXiv:1705.05370 [hep-ph]].
- [77] L. Di Luzio, F. Mescia, E. Nardi, P. Panci and R. Ziegler, Phys. Rev. Lett. **120**, no. 26, 261803 (2018) doi:10.1103/PhysRevLett.120.261803 [arXiv:1712.04940 [hep-ph]].
- [78] H. P. Nilles and S. Raby, Nucl. Phys. B **198**, 102 (1982). doi:10.1016/0550-3213(82)90547-8
- [79] M. B. Wise, H. Georgi and S. L. Glashow, Phys. Rev. Lett. **47**, 402 (1981). doi:10.1103/PhysRevLett.47.402
- [80] S. M. Boucenna and Q. Shafi, Phys. Rev. D **97**, no. 7, 075012 (2018) doi:10.1103/PhysRevD.97.075012 [arXiv:1712.06526 [hep-ph]].
- [81] A. Ernst, A. Ringwald and C. Tamarit, JHEP **1802**, 103 (2018) doi:10.1007/JHEP02(2018)103 [arXiv:1801.04906 [hep-ph]].
- [82] A. G. Dias, A. C. B. Machado, C. C. Nishi, A. Ringwald and P. Vaudrevange, JHEP **1406**, 037 (2014) doi:10.1007/JHEP06(2014)037 [arXiv:1403.5760 [hep-ph]].
- [83] G. Ballesteros, J. Redondo, A. Ringwald and C. Tamarit, Phys. Rev. Lett. **118**, no. 7, 071802 (2017) doi:10.1103/PhysRevLett.118.071802 [arXiv:1608.05414 [hep-ph]].
- [84] E. Ma, T. Ohata and K. Tsumura, Phys. Rev. D **96**, no. 7, 075039 (2017) doi:10.1103/PhysRevD.96.075039 [arXiv:1708.03076 [hep-ph]].
- [85] Y. Chikashige, R. N. Mohapatra and R. D. Peccei, Phys. Lett. **98B**, 265 (1981). doi:10.1016/0370-2693(81)90011-3
- [86] G. B. Gelmini and M. Roncadelli, Phys. Lett. **99B**, 411 (1981). doi:10.1016/0370-2693(81)90559-1
- [87] F. Wilczek, Phys. Rev. Lett. **49**, 1549 (1982). doi:10.1103/PhysRevLett.49.1549
- [88] Z. G. Berezhiani and M. Y. Khlopov, Sov. J. Nucl. Phys. **51**, 739 (1990) [Yad. Fiz. **51**, 1157 (1990)].
- [89] J. Jaeckel, Phys. Lett. B **732**, 1 (2014) doi:10.1016/j.physletb.2014.03.005 [arXiv:1311.0880 [hep-ph]].
- [90] F. Arias-Aragon and L. Merlo, JHEP **1710**, 168 (2017) doi:10.1007/JHEP10(2017)168 [arXiv:1709.07039 [hep-ph]].
- [91] M.B. Green, J.H. Schwarz, E. Witten, Superstring Theory, Volume 1: Introduction, Superstring Theory, Volume 2: Loop Amplitudes, Anomalies and Phenomenology, Cambridge University Press, 1987.
- [92] Joseph Polchinski, String Theory Vol. I: An Introduction to the Bosonic String, String Theory Vol. II: Superstring Theory and Beyond, Cambridge University Press, 1998.
- [93] K. Becker, M. Becker, J.H. Schwarz, String Theory and M-Theory, Cambridge University Press, 2007.
- [94] P. Candelas, G. T. Horowitz, A. Strominger and E. Witten, Nucl. Phys. B **258**, 46 (1985). doi:10.1016/0550-3213(85)90602-9
- [95] P. Svrcek and E. Witten, JHEP **0606**, 051 (2006) doi:10.1088/1126-6708/2006/06/051 [hep-th/0605206].
- [96] A. Arvanitaki, S. Dimopoulos, S. Dubovsky, N. Kaloper and J. March-Russell, Phys. Rev. D **81**, 123530 (2010) doi:10.1103/PhysRevD.81.123530 [arXiv:0905.4720 [hep-th]].
- [97] J. Preskill, M. B. Wise and F. Wilczek, Phys. Lett. B **120**, 127 (1983) [Phys. Lett. **120B**, 127 (1983)]. doi:10.1016/0370-2693(83)90637-8
- [98] L. F. Abbott and P. Sikivie, Phys. Lett. B **120**, 133 (1983) [Phys. Lett. **120B**, 133 (1983)]. doi:10.1016/0370-2693(83)90638-X
- [99] M. Dine and W. Fischler, Phys. Lett. B **120**, 137 (1983) [Phys. Lett. **120B**, 137 (1983)]. doi:10.1016/0370-2693(83)90639-1
- [100] J. E. Kim, Phys. Rept. **150**, 1 (1987). doi:10.1016/0370-1573(87)90017-2
- [101] P. Sikivie, Lect. Notes Phys. **741**, 19 (2008) doi:10.1007/978-3-540-73518-2_2 [astro-ph/0610440].
- [102] M. Srednicki, Nucl. Phys. B **260**, 689 (1985). doi:10.1016/0550-3213(85)90054-9
- [103] G. W. Gibbons and S. W. Hawking, Phys. Rev. D **15**, 2738 (1977). doi:10.1103/PhysRevD.15.2738
- [104] P. A. R. Ade *et al.* [BICEP2 and Planck Collaborations], Phys. Rev. Lett. **114**, 101301 (2015) doi:10.1103/PhysRevLett.114.101301 [arXiv:1502.00612 [astro-ph.CO]].
- [105] B. S. Acharya, K. Bobkov and P. Kumar, JHEP **1011**, 105 (2010) doi:10.1007/JHEP11(2010)105 [arXiv:1004.5138 [hep-th]].
- [106] M. Cicoli, J. P. Conlon and F. Quevedo, Phys. Rev. D **87**, no. 4, 043520 (2013) doi:10.1103/PhysRevD.87.043520 [arXiv:1208.3562 [hep-ph]].
- [107] T. Higaki and F. Takahashi, JHEP **1211**, 125 (2012) doi:10.1007/JHEP11(2012)125 [arXiv:1208.3563 [hep-ph]].
- [108] T. Higaki, K. Nakayama and F. Takahashi, JHEP **1307**, 005 (2013) doi:10.1007/JHEP07(2013)005 [arXiv:1304.7987 [hep-ph]].
- [109] J. P. Conlon and M. C. D. Marsh, JHEP **1310**, 214 (2013) doi:10.1007/JHEP10(2013)214 [arXiv:1304.1804 [hep-ph]].
- [110] T. W. B. Kibble, J. Phys. A **9**, 1387 (1976). doi:10.1088/0305-4470/9/8/029
- [111] T. Hiramatsu, M. Kawasaki, K. Saikawa and T. Sekiguchi, Phys. Rev. D **85**, 105020 (2012) Erratum: [Phys. Rev. D **86**, 089902 (2012)] doi:10.1103/PhysRevD.86.089902, 10.1103/PhysRevD.85.105020 [arXiv:1202.5851 [hep-ph]].
- [112] S. M. Barr and J. E. Kim, Phys. Rev. Lett. **113**, no. 24, 241301 (2014) doi:10.1103/PhysRevLett.113.241301 [arXiv:1407.4311 [hep-ph]].
- [113] E.W. Kolb, M.S. Turner, The Early Universe, Addison-Wesley, 1990.
- [114] Q. Yang and H. Di, Phys. Rev. D **95**, no. 7, 075032 (2017) doi:10.1103/PhysRevD.95.075032 [arXiv:1610.08378 [hep-ph]].
- [115] T. Oniga and C. H.-T. Wang, Phys. Rev. D **94**, no. 6, 061501 (2016) doi:10.1103/PhysRevD.94.061501 [arXiv:1603.09193 [gr-qc]].
- [116] S. S. Chakrabarty, S. Enomoto, Y. Han, P. Sikivie and E. M. Todarello, Phys. Rev. D **97** (2018) no.4, 043531 [arXiv:1710.02195 [hep-ph]].
- [117] K. Saikawa and M. Yamaguchi, Phys. Rev. D **87** (2013) no.8, 085010 [arXiv:1210.7080 [hep-ph]].
- [118] S. Davidson and M. Elmer, JCAP **1312** (2013) 034 [arXiv:1307.8024 [hep-ph]].
- [119] S. Davidson, Astropart. Phys. **65** (2015) 101 [arXiv:1405.1139 [hep-ph]].

- [120] A. H. Guth, M. P. Hertzberg and C. Prescod-Weinstein, Phys. Rev. D **92** (2015) no.10, 103513 [arXiv:1412.5930 [astro-ph.CO]].
- [121] S. Seager, D. D. Sasselov and D. Scott, Astrophys. J. **523** (1999) L1 [astro-ph/9909275].
- [122] P. W. Graham, I. G. Irastorza, S. K. Lamoreaux, A. Lindner and K. A. van Bibber, Ann. Rev. Nucl. Part. Sci. **65** (2015) 485 [arXiv:1602.00039 [hep-ex]].
- [123] G. G. Raffelt, Chicago, USA: Univ. Pr. (1996) 664 p
- [124] M. Archidiacono, S. Hannestad, A. Mirizzi, G. Raffelt and Y. Y. Y. Wong, JCAP **1310** (2013) 020 [arXiv:1307.0615 [astro-ph.CO]].
- [125] M. Archidiacono, T. Basse, J. Hamann, S. Hannestad, G. Raffelt and Y. Y. Y. Wong, JCAP **1505** (2015) no.05, 050 [arXiv:1502.03325 [astro-ph.CO]].
- [126] M. Giannotti, I. G. Irastorza, J. Redondo, A. Ringwald and K. Saikawa, JCAP **1710**, no. 10, 010 (2017) doi:10.1088/1475-7516/2017/10/010 [arXiv:1708.02111 [hep-ph]].
- [127] J. S. Lee, arXiv:1808.10136 [hep-ph].
- [128] M. Hindmarsh and P. Moulatsiotis, Phys. Rev. D **56** (1997) 8074 [hep-ph/9708281].
- [129] G. B. Zhao *et al.*, Mon. Not. Roy. Astron. Soc. **457**, no. 3, 2377 (2016) doi:10.1093/mnras/stw135 [arXiv:1510.08216 [astro-ph.CO]].
- [130] M. Ata *et al.*, Mon. Not. Roy. Astron. Soc. **473**, no. 4, 4773 (2018) doi:10.1093/mnras/stx2630 [arXiv:1705.06373 [astro-ph.CO]].
- [131] R. D. Peccei, Lect. Notes Phys. **741**, 3-17 (2008) doi:10.1007/978-3-540-73518-2-1 [arXiv:hep-ph/0607268 [hep-ph]].
- [132] J. E. Kim and G. Carosi, Rev. Mod. Phys. **82**, 557-602 (2010) doi:10.1103/RevModPhys.82.557 [arXiv:0807.3125 [hep-ph]].
- [133] M. Dine, [arXiv:hep-ph/0011376 [hep-ph]].
- [134] I. G. Irastorza and J. Redondo, Prog. Part. Nucl. Phys. **102**, 89-159 (2018) doi:10.1016/j.ppnp.2018.05.003 [arXiv:1801.08127 [hep-ph]].